γγ Simulations for XCC and 15 TeV

Multi-TeV Beam-Beam Meeting

Tim Barklow

Jan 19, 2024

SLAC NATIONAL ACCELERATOR LABORATORY

Stanford University | U.S. DEPARTMENT OF ENERGY

$\gamma\gamma$ Collider Basics

Photon Collider Basics

Photons from a high powered laser are scattered off the high energy beam electrons of a linear collider between the final quadrupole and the interaction point. The compton scattered photons acquire the momenta of the high energy electrons and collide at the i.p. with the compton scattered photons from the opposing beam. The $\gamma\gamma$ luminosity will be given by the geometric e^+e^- luminosity times the compton conversion efficiency squared.

$$x = \frac{4E_{e^-}\omega_0}{m_e^2} \qquad \omega = \frac{\omega_m}{1+\left(\theta/\theta_0\right)^2} \qquad \omega_m = \frac{x}{x+1}E_{e^-} \qquad \theta_0 = \frac{m_e}{E_{e^-}}\sqrt{x+1}$$

$m_e^2(x+1) =$ center of mass energy squared of electron and laser photon

$\omega_0 =$ laser photon energy

$\omega =$ compton scattered (high energy) photon energy

$\theta =$ angle of compton scattered (high energy) photon w.r.t. electron

P_c = mean helicity of laser beam $|P_c| \le 1$

λ_e = mean helicity of electron beam $|\lambda_e| \le \frac{1}{2}$

ξ_i = mean helicity of the high energy photon beam i, i=1,2 $|\xi_i| \le 1$

The thresholds for two important physics processes are crossed as x is varied:

At $x = 4.82$ $\gamma\gamma_{\text{laser}} \to e^+e^-$ opens up which depletes the high energy photon beam

At $x = 8$ $e^-\gamma_{\text{laser}} \to e^+e^-e^-$ opens up. This process smears the electron energy and hence smears the high energy photon spectrum.

Both of these effects are included in the CAIN MC simulation.

Nominal configuration with optical laser

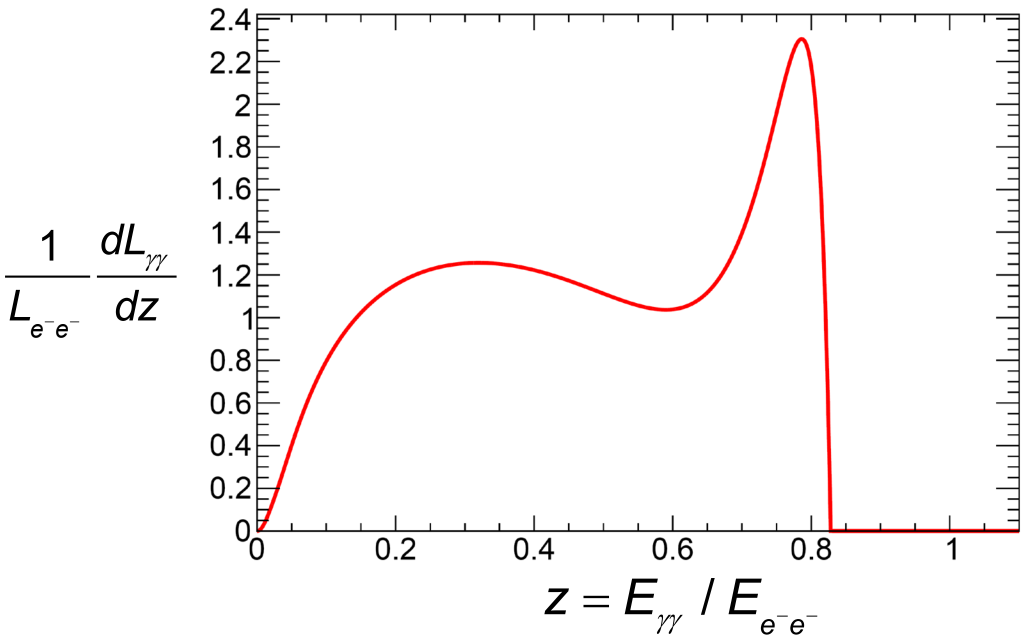

$x = 4.82 \quad E_{e^-e^-} = 158$ GeV $\quad \kappa = 1$

pol$(e^-) = 90\% \quad 2P_c\lambda_e = -0.9 \quad h\nu = 3.98$ eV

(κ= 1 − prob that γ annihilates with laser γ)

$$\int dz \frac{1}{L_{e^-e^-}}\frac{dL_{\gamma\gamma}}{dz}\sigma(\gamma\gamma \to H) = 247 \text{ fb}$$

Start increasing photon energy (x value) ...

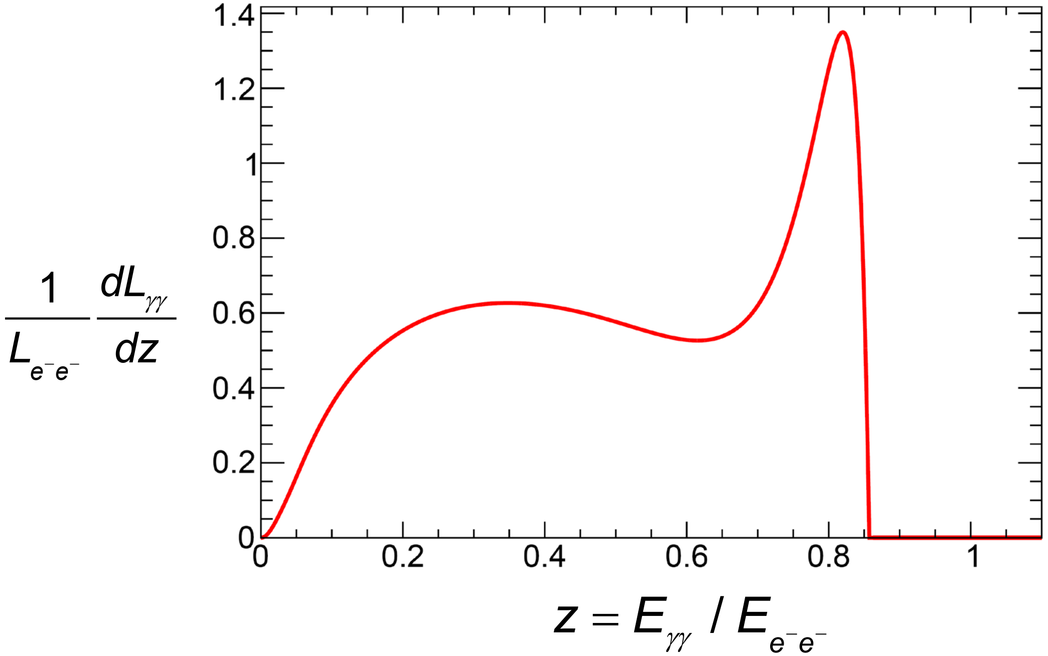

$x = 6.00 \quad E_{e^-e^-} = 150$ GeV $\quad \kappa = 0.73$

pol$(e^-) = 90\% \quad 2P_c\lambda_e = -0.9 \quad h\nu = 5.22$ eV

$$\int dz \frac{1}{L_{e^-e^-}}\frac{dL_{\gamma\gamma}}{dz}\sigma(\gamma\gamma \to H) = 130 \text{ fb}$$

Keep increasing photon energy (x value) ...

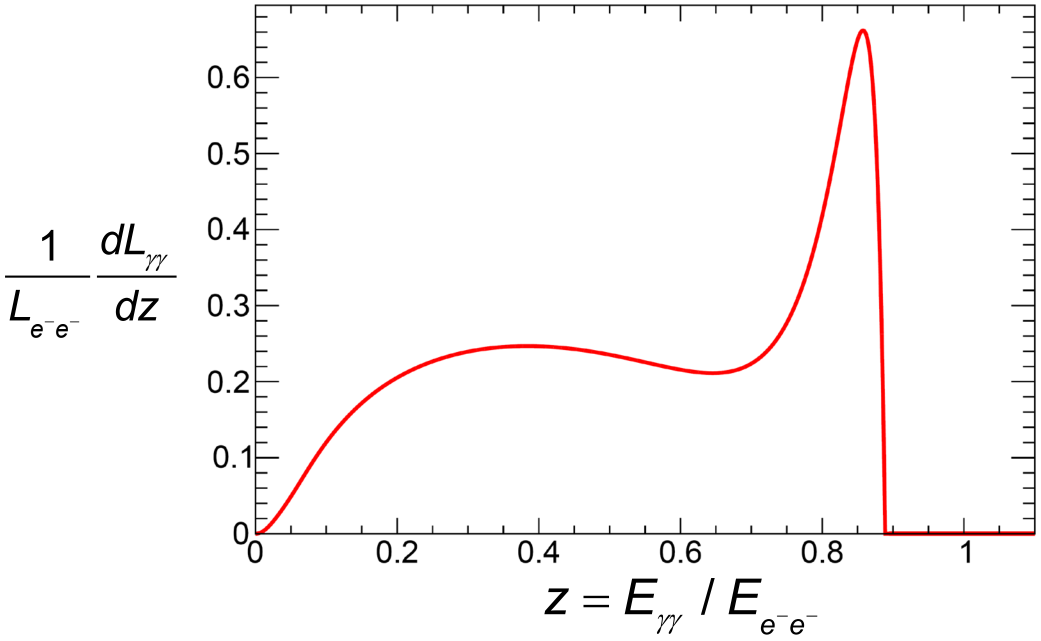

$x = 8.00 \quad E_{e^-e^-} = 146.5\ \text{GeV} \quad \kappa = 0.48$

$\text{pol}(e^-) = 90\% \quad 2P_c\lambda_e = -0.9$

$$\int dz \frac{1}{L_{e^-e^-}} \frac{dL_{\gamma\gamma}}{dz} \sigma(\gamma\gamma \to H) = 78\ \text{fb}$$

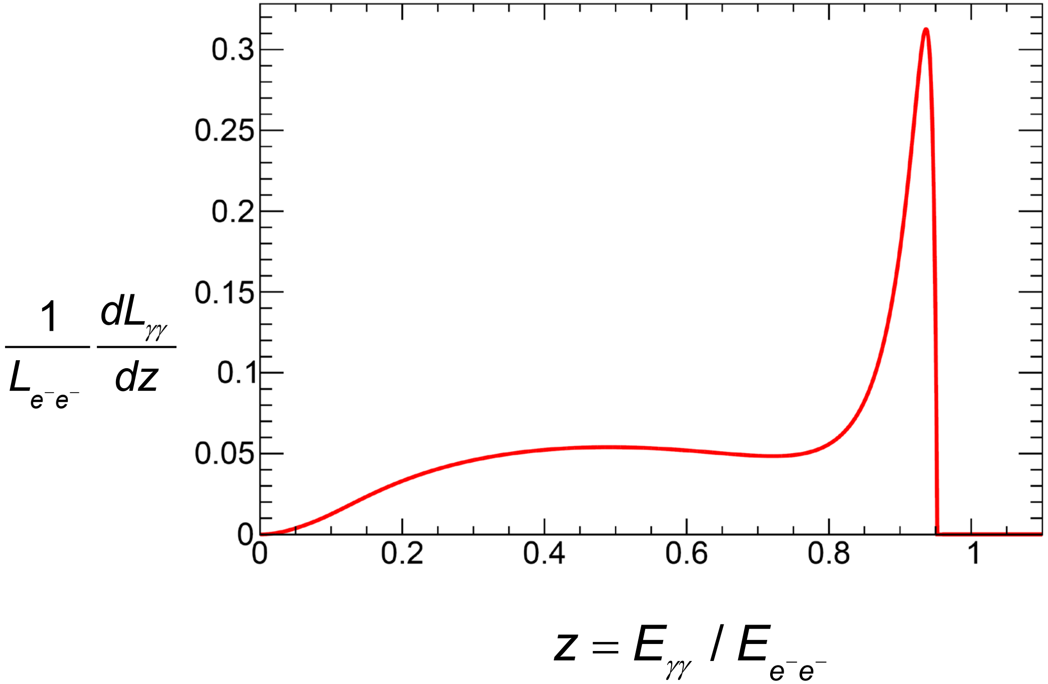

$x = 20.00 \quad E_{e^-e^-} = 134.8\ \text{GeV} \quad \kappa = 0.25$

$\text{pol}(e^-) = 90\% \quad 2P_c\lambda_e = -0.9$

$$\int dz \frac{1}{L_{e^-e^-}} \frac{dL_{\gamma\gamma}}{dz} \sigma(\gamma\gamma \to H) = 40\ \text{fb}$$

Keep increasing photon energy (x value) ...

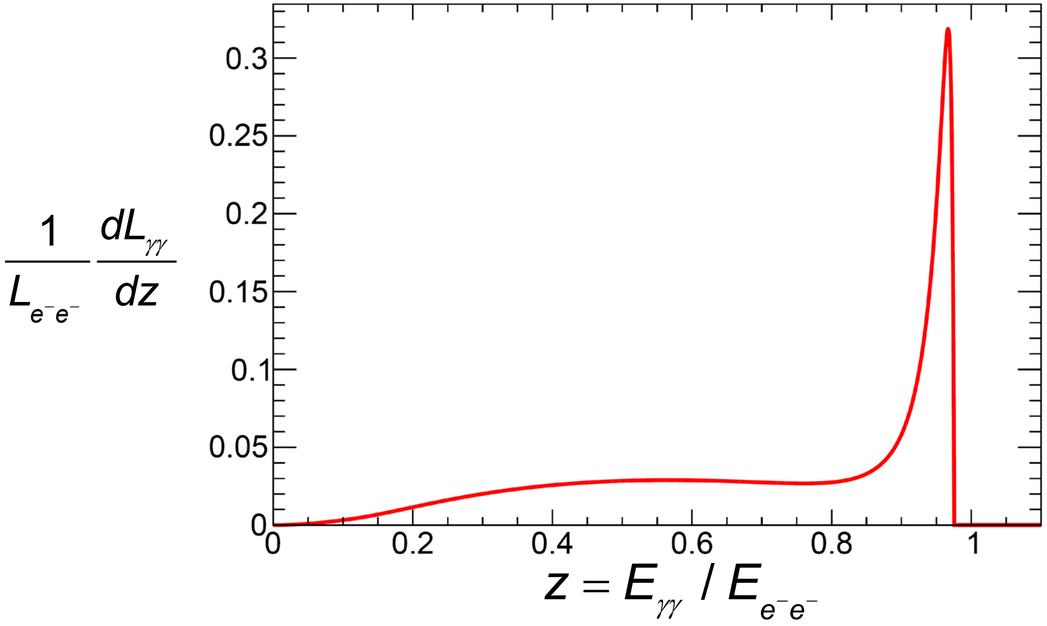

$x = 40.00 \quad E_{e^-e^-} = 130.3$ GeV $\quad \kappa = 0.19$

$\mathrm{pol}(e^-) = 90\% \quad 2P_c\lambda_e = -0.9$

$$\int dz \frac{1}{L_{e^-e^-}} \frac{dL_{\gamma\gamma}}{dz} \sigma(\gamma\gamma \to H) = 42 \text{ fb}$$

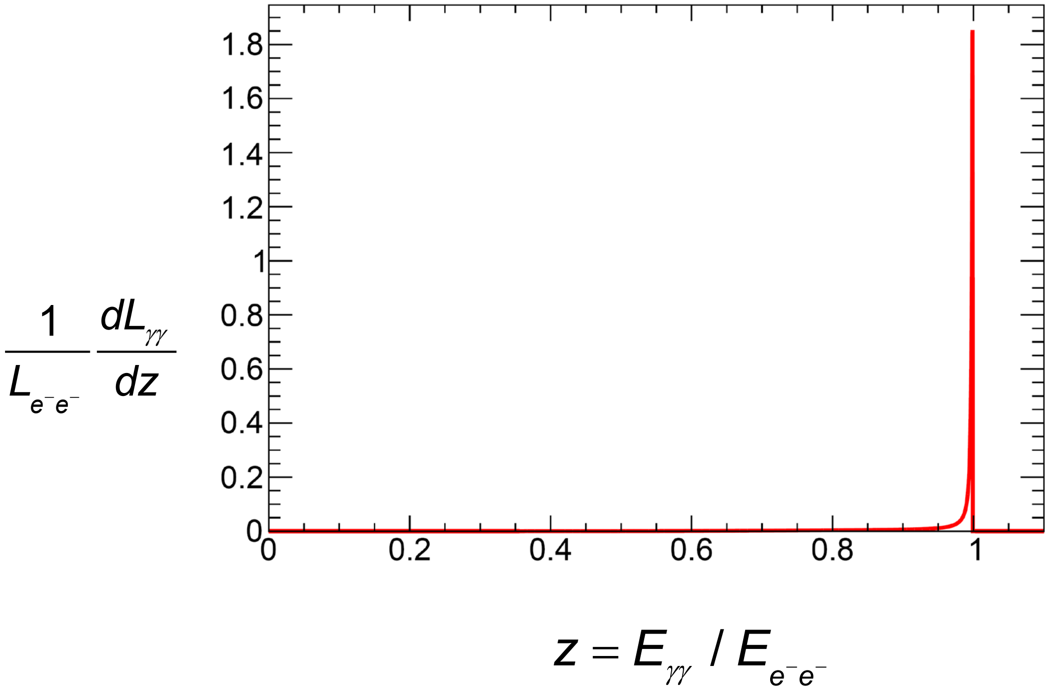

$x = 1000. \quad E_{e^-e^-} = 126.2$ GeV $\quad \kappa = 0.11$

$\mathrm{pol}(e^-) = 90\% \quad 2P_c\lambda_e = -0.9$

$$\int dz \frac{1}{L_{e^-e^-}} \frac{dL_{\gamma\gamma}}{dz} \sigma(\gamma\gamma \to H) = 257 \text{ fb}$$

At large x values the opposite $e^-\gamma$ helicity product sign also gives peaked lumi spectrum

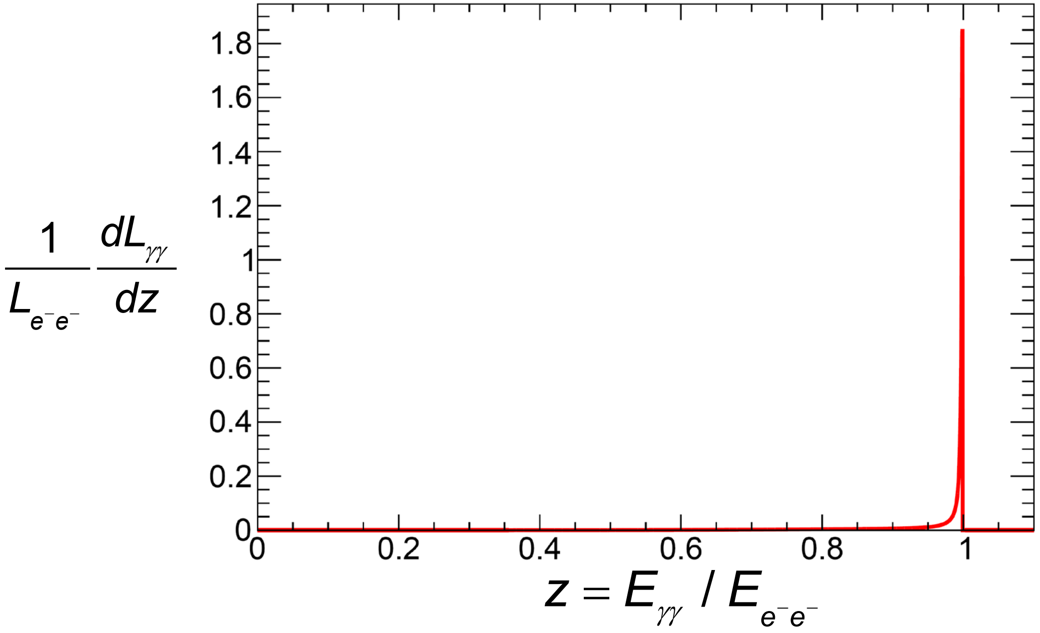

$x = 1000.$ $E_{e^-e^-} = 125.2$ GeV κ=0.11

pol(e^-) = 90% $2P_c\lambda_e = -0.9$

$$\int dz \frac{1}{L_{e^-e^-}} \frac{dL_{\gamma\gamma}}{dz} \sigma(\gamma\gamma \to H) = 257 \text{ fb}$$

$x = 1000$ with $2P_c\lambda_e = +0.9$ is baseline XCC due to higher Higgs rate. Detailed detector/physics studies will determine which of $2P_c\lambda_e = \pm 0.9$ is better.

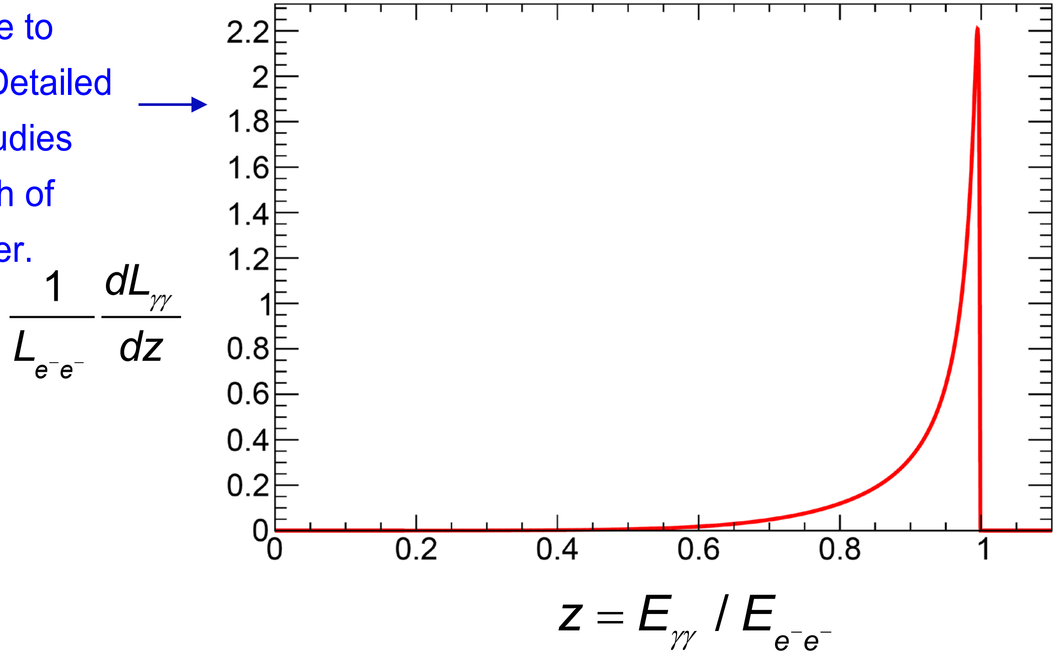

$x = 1000.$ $E_{e^-e^-} = 125.6$ GeV κ=0.44

pol(e^-) = 90% $2P_c\lambda_e = +0.9$ $h\nu = 1.03$ keV

$$\int dz \frac{1}{L_{e^-e^-}} \frac{dL_{\gamma\gamma}}{dz} \sigma(\gamma\gamma \to H) = 311 \text{ fb}$$

$2P_c\lambda_e = +0.9$ gives broader spectrum in $E_{\gamma\gamma}$ but this is compensated by suppression of $\gamma\gamma \to e^+e^-$ (κ=0.44 vs 0.11 for opposite sign of $2P_c\lambda_e$)

XCC

XCC

XCC s-channel $\gamma\gamma \to H$ @ $\sqrt{s} = 125$ GeV

$\gamma\gamma \to HH$ @ $\sqrt{s} = 380$ GeV

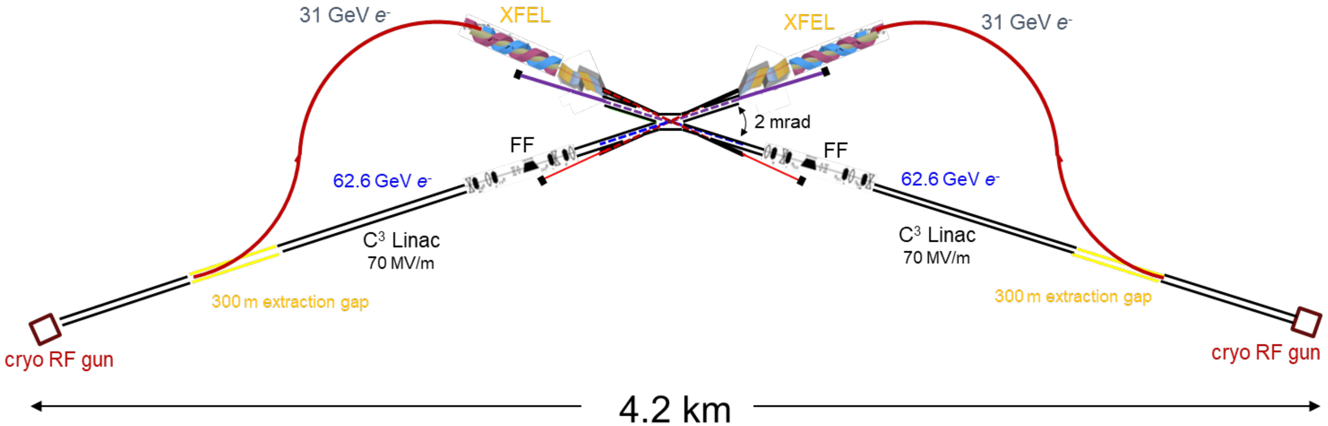

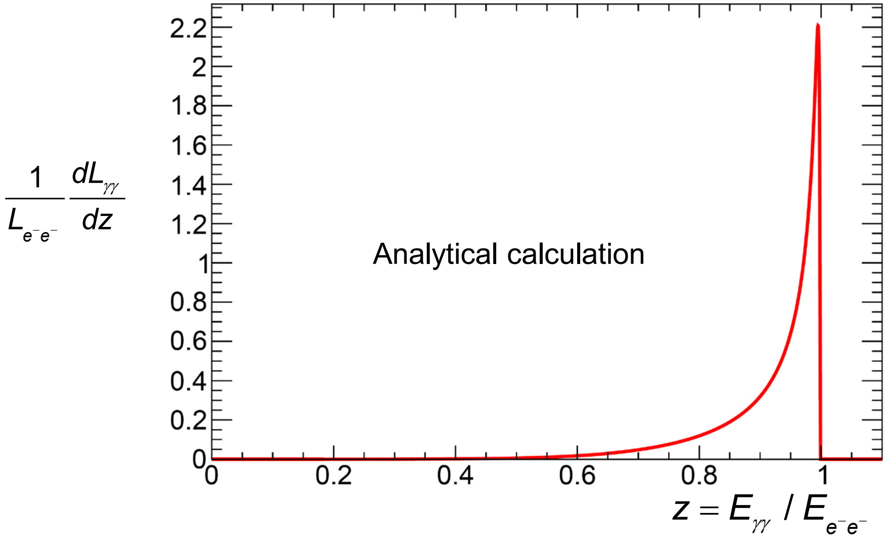

Final Focus parameters	Approx. value	XFEL parameters	Approx. value
Electron energy	62.8 GeV	Electron energy	31 GeV
Electron beam power	0.57 MW	Electron beam power	0.28 MW
β_x/β_y	0.03/0.03 mm	normalized emittance	120 nm
$\gamma\epsilon_x/\gamma\epsilon_y$	120/120 nm	RMS energy spread $\langle\Delta\gamma/\gamma\rangle$	0.05%
σ_x/σ_y at e^-e^- IP	5.4/5.4 nm	bunch charge	1 nC
σ_z	20 μm	Linac-to-XFEL curvature radius	133 km
bunch charge	1 nC	Undulator B field	$\gtrsim$ 1 T
Rep. Rate at IP	240 × 38 Hz	Undulator period λ_u	9 cm
σ_x/σ_y at IPC	12.1/12.12 nm	Average β function	12 m
$\mathcal{L}_{\text{geometric}}$	9.7×10^{34} cm^2 s^{-1}	x-ray λ (energy)	1.2 nm (1 keV)
δ_E/E	0.05%	x-ray pulse energy	0.7 J
L^* (QD0 exit to e^- IP)	1.5m	pulse length	40 μm
d_{cp} (IPC to IP)	60 μm	$a_{\gamma x}/a_{\gamma y}$ (x/y waist)	21.2/21.2 nm
QD0 aperture	9 cm diameter	non-linear QED ξ^2	0.10

Site parameters	Approx. value		
crossing angle	2 mrad		
total site power	85 MW		
total length	3.0 km		

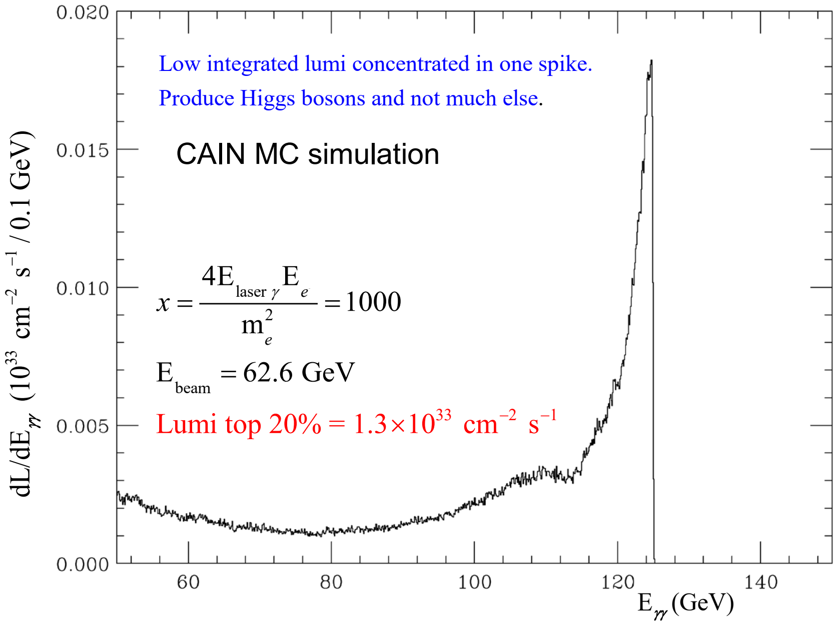

XCC

XCC s-channel $\gamma\gamma \to H$ @ $\sqrt{s} = 125$ GeV

$\gamma\gamma \to HH$ @ $\sqrt{s} = 380$ GeV

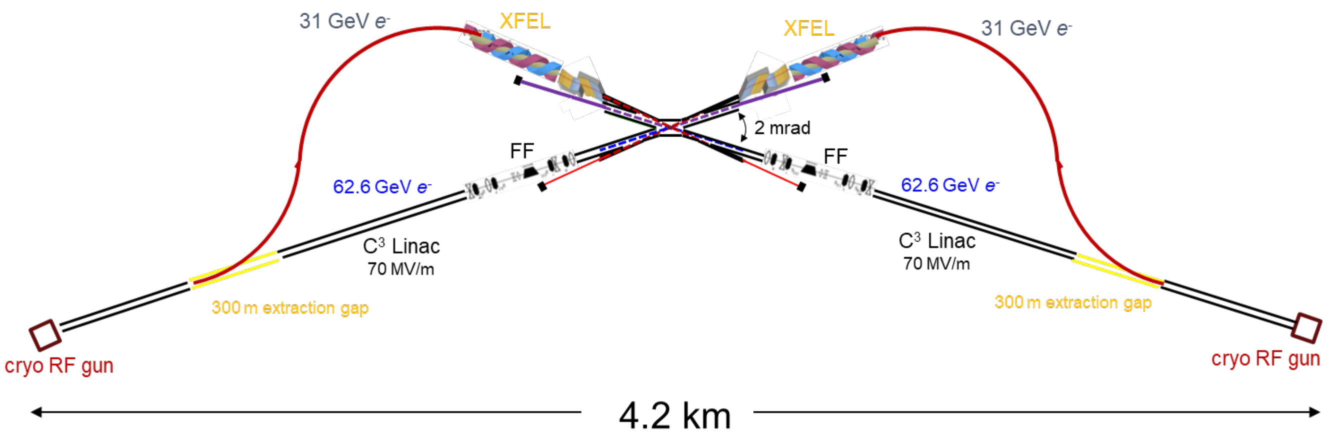

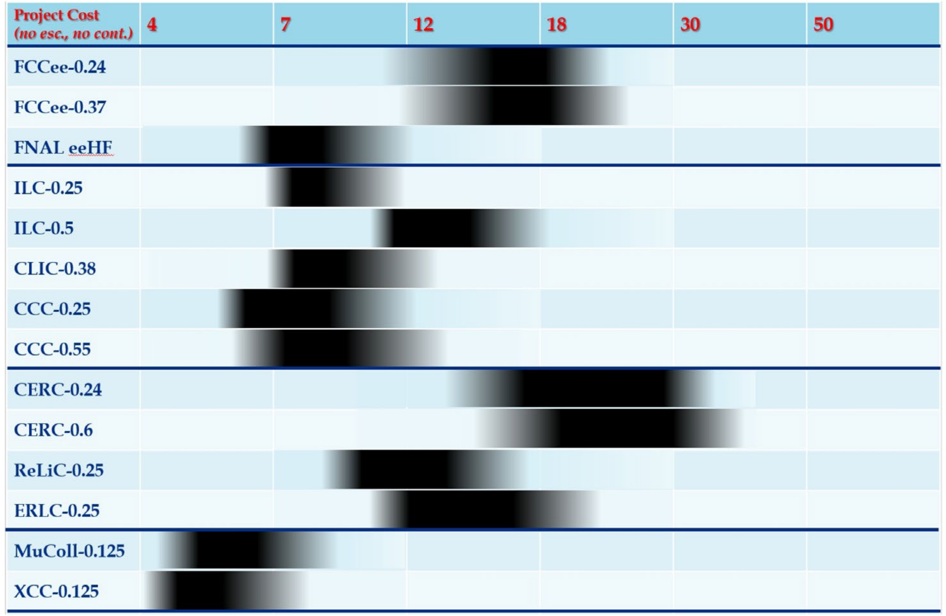

ITF

4.2 km accommodates $\sqrt{s}$=380 GeV with 120 MV/m.

- The $\gamma\gamma$ luminosity is $L_{\gamma\gamma} = L_{ee}\kappa^2$ where L_{ee} is the e^-e^- luminosity and κ is the Compton conversion efficiency.
- $\kappa = 0.2,$ so XCC is basically an e^-e^- collider with just enough converted photons to produce 80,000 Higgs/year
- The e^-e^- luminosity -- and therefore the $\gamma\gamma$ luminosity -- is optimized and maintained using e^-e^- beam-beam deflection and beamstrahlung monitors (just like ILC/C^3)
- The unique interaction region pieces are the two Compton IP's, located 60 μm upstream of the e^-e^- IP, where collisions between the e^- and X-ray beams must be maintained to keep $\kappa \approx 0.2$.

The XCC is very different from previous γγ collider concepts

Machine	E_{e^-} (GeV)	Polarization	N_H/yr	N_{Bgnd}/N_H	$N_{pileup/BX}$
XCC	62.8	90% e^-	80,000	170	1.3
2.4 eV laser	86.5	90% e^-	52,000	1310	6.8
ILC	125	−80% e^- +30% e^+	98,000	130	1.3
ILC	125	+80% e^- −30% e^+	65,000	50	1.3

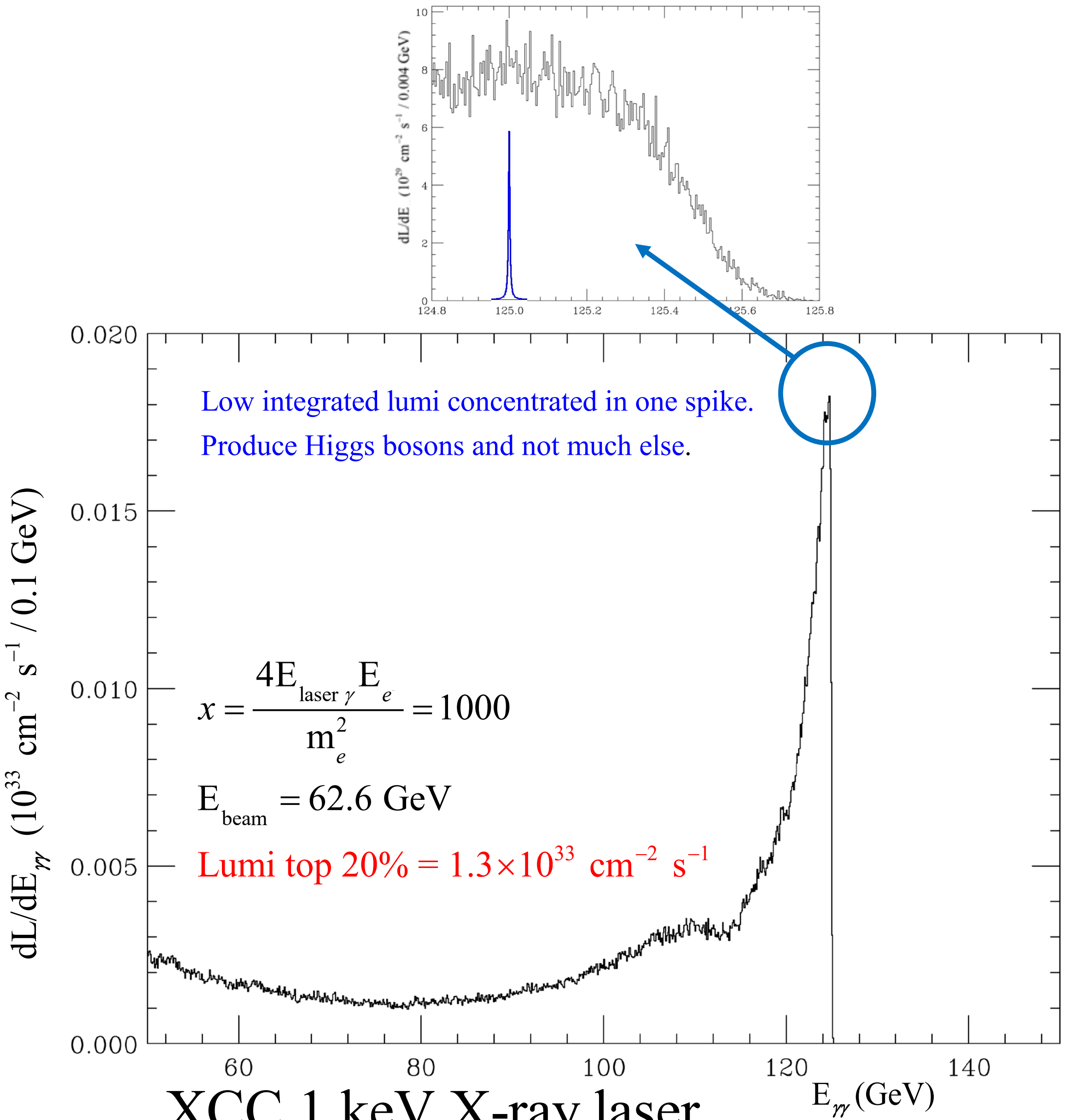

XCC 1 keV X-ray laser

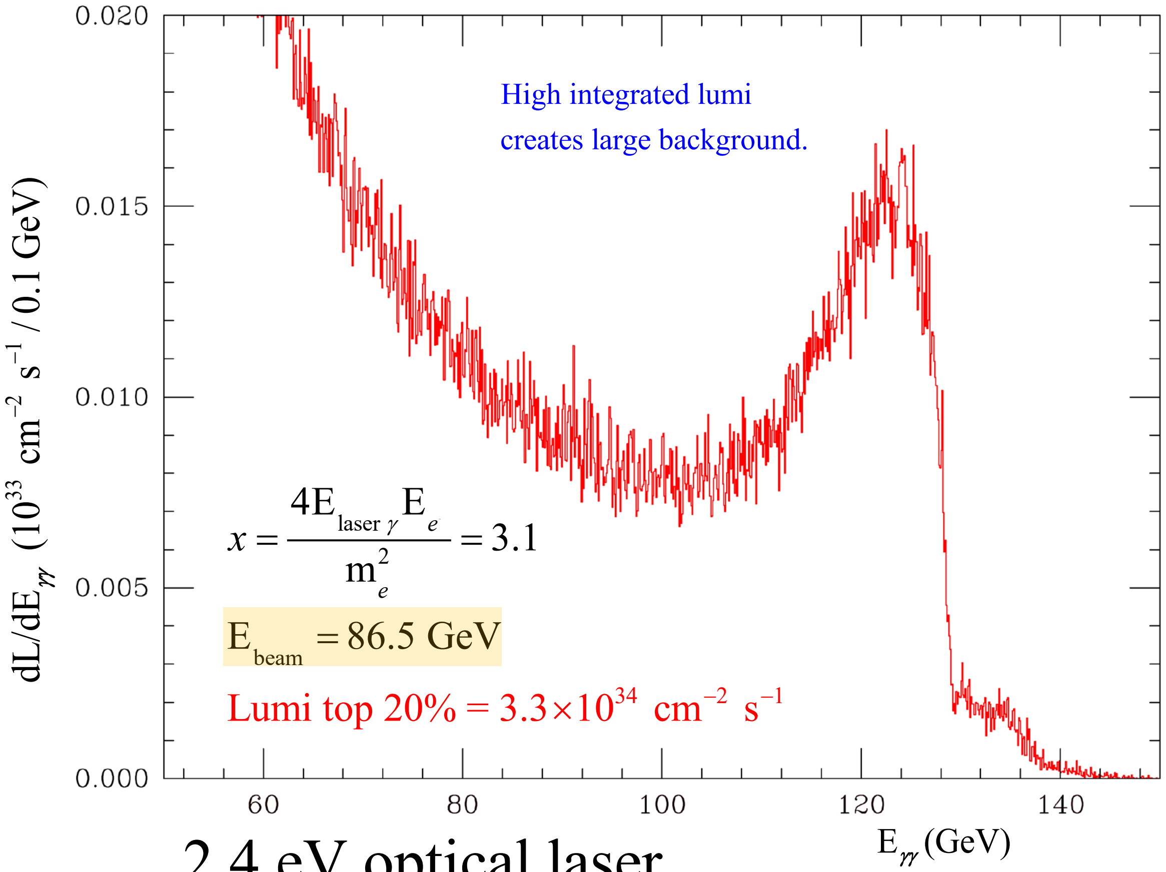

2.4 eV optical laser

ILC/C^3 vs. XCC Physics Comparison

Stage I & II Parameters

Colliding Particles	ILC/C^3 e^+e^-	XCC $\gamma\gamma$
Stage I:		
$\sqrt{s}$ (GeV)	250	125
Luminosity (fb^{-1})	2000	460
Beam Power (MW)	5.3 / 4.0	4.0
Run Time (yr)	10	10
# Single Higgs	0.5×10^6	1.3×10^6
Stage II:		
$\sqrt{s}$ (GeV)	550	380
Luminosity (fb^{-1})	4000	4900
Beam Power (MW)	11 / 4.9	4.9
Run Time (yr)	10	10
# Single Higgs (I+II)	1.5×10^6	1.3×10^6
# Double Higgs	840	1800
# $t\bar{t}$	2.0×10^6	2.9×10^6

Stage I, 10 years

κ framework BR$_{\text{BSM}} = 0$

coupling a	HL-LHC† Δa (%)	ILC/C^3 Δa (%)	XCC Δa (%)
HZZ	2.4	0.46	0.83
HWW	2.6	0.44	0.84
Hbb	6.0	0.83	0.85
$H\tau\tau$	2.8	0.98	0.89
Hgg	4.0	1.6	1.1
Hcc	-	1.8	1.2
$H\gamma\gamma$	2.9	1.1	0.10
$H\gamma Z$	-	-	1.5
$H\mu\mu$	6.7	4.0	3.5
Γ_{tot}	5	1.6	1.7

† S1 from Table 36 in arXiv:1902.00134 [hep-ph]

Stage I+II, 20 years

Model Independent EFT

coupling a	ILC/C^3 Δa (%)	XCC # Δa (%)
HZZ	0.38	0.94
HWW	0.37	0.94
Hbb	0.60	0.95
$H\tau\tau$	0.77	0.99
Hgg	0.96	1.2
Hcc	1.2	1.2
$H\gamma\gamma$	1.0	0.44
$H\gamma Z$	4.0	1.5
$H\mu\mu$	3.8	3.5
Htt	2.8	4.6
HHH	20	14*
Γ_{tot}	1.6	2.4
Γ_{inv} †	0.32	–
Γ_{other} †	1.3	1.5

† 95% C.L. limit

*assumes XCC error is ILC/C^3 value scaled by $1/\sqrt{N_{HH}}$

#XCC achieves model independence through measurement of $\Gamma_{\gamma\gamma}$ using monochomatic electron in $e^-\gamma \rightarrow e^- H$ during $\sqrt{s} = 380$ GeV $\gamma\gamma$ run.

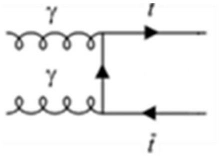
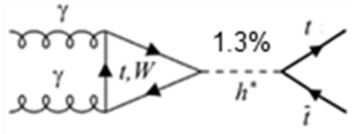

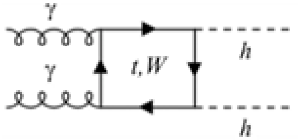
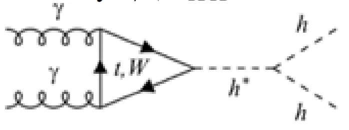

XCC and P5

The recent P5 report calls out C3 accelerator R&D but does not mention a C3-based collider concept. The report discusses a 2028 P5 Higgs factory review but doesn't specify the initial state of the Higgs factory collider. With respect to P5 then, the XCC should be considered primarily as an onshore Higgs Factory to be reviewed by the 2028 P5 subpanel. Secondarily it is a prototype for a 10 TeV pCM $\gamma\gamma$ collider.

XCC advantages:

- $\approx$ 40% lower cost w.r.t C3
- Highly synergistic with SLAC XFEL program.
- XCC has a factor of 2 statistical advantage w.r.t. ILC/C^3 in double Higgs production, and may have additional advantages in the triple Higgs coupling measurement due to the simplicity of the HH final state vs. ZHH.
- Physics would be more complementary to CEPC than ILC/C^3, generally due to a different initial state, and specifically due to enhanced $\Delta H\gamma\gamma$, $\Delta H\gamma Z$ & ΔHHH precision.
- If positron acceleration is a show stopper for a 10 TeV PWFA e^+e^- collider then the PWFA must be operated in $\gamma\gamma$ mode, in which case XCC would serve as a $\gamma\gamma$ collider prototype (in this respect it may be possible for the XCC to tap into some of the 10 TeV pCM collider R&D P5 support)

XCC and P5

XCC challenges:

- e^- accelerator with $70-120$ MV/m (common with C^3 e^+e^- collider)
- Polarized low emittance e^- injector (common with C^3 e^+e^-, except flat beams not needed)
- Focusing of round e^- beams to $\sigma_{x,y} = 5.5$ nm
- Production and focusing of 1 keV γ XFEL with 700 mJ/pulse to 70 nm FWHM waist
- XFEL and e^- beamline layouts around the IP
- Timing stability of the XFEL laser beam and e^- beam at Compton IP.

Simulation of 15 TeV $\gamma\gamma$ Collider

Replace 62.5 GeV C^3 e- beam w/ 7500 GeV PWFA e- beam and simulate $\gamma\gamma$ Collisions using CAIN MC

Technology	PWFA	$\gamma\gamma$ PWFA
Aspect Ratio	Round	Round
CM Energy	15	15
Single beam energy (TeV)	7.5	7.5
Gamma	1.47E+07	1.4E+07
Emittance X (mm mrad)	0.1	0.12
Emittance Y (mm mrad)	0.1	0.12
Beta* X (m)	1.50E-04	0.30E-04
Beta* Y (m)	1.50E-04	0.30E-04
Sigma* X (nm)	1.01	0.48
Sigma* Y (nm)	1.01	0.48
N_bunch (num)	5.00E+09	6.2E+09 (or 5.00E+09)
Freq (Hz)	7725	7725
Sigma Z (um)	5	5
Geometric Lumi ($cm^{-2}\ s^{-1}$)	1.50E+36	6.58E+36

Start with x=4.8 because this was considered the typical $\gamma\gamma$ collider x value before this study was performed

x=4.8 adjust parameters to get ~ 100 % conversion w/ linear QED

$x = 4.8 \;\Rightarrow\; 9100$ GeV $e^- + 0.034$ eV γ (λ=36 μm) $a_{\gamma FWHM} = 2.1$ mm $\sigma_{\gamma z} = 0.79$ mm $d_{cp} = 2.4$ mm

$\sigma_{ez} = 5\ \mu$m N_{e^-} =1 nC $\gamma\varepsilon_{x,y} = 120$ nm $2P_c\lambda_e = -0.9$ $E_{pulse} = 4400$ J

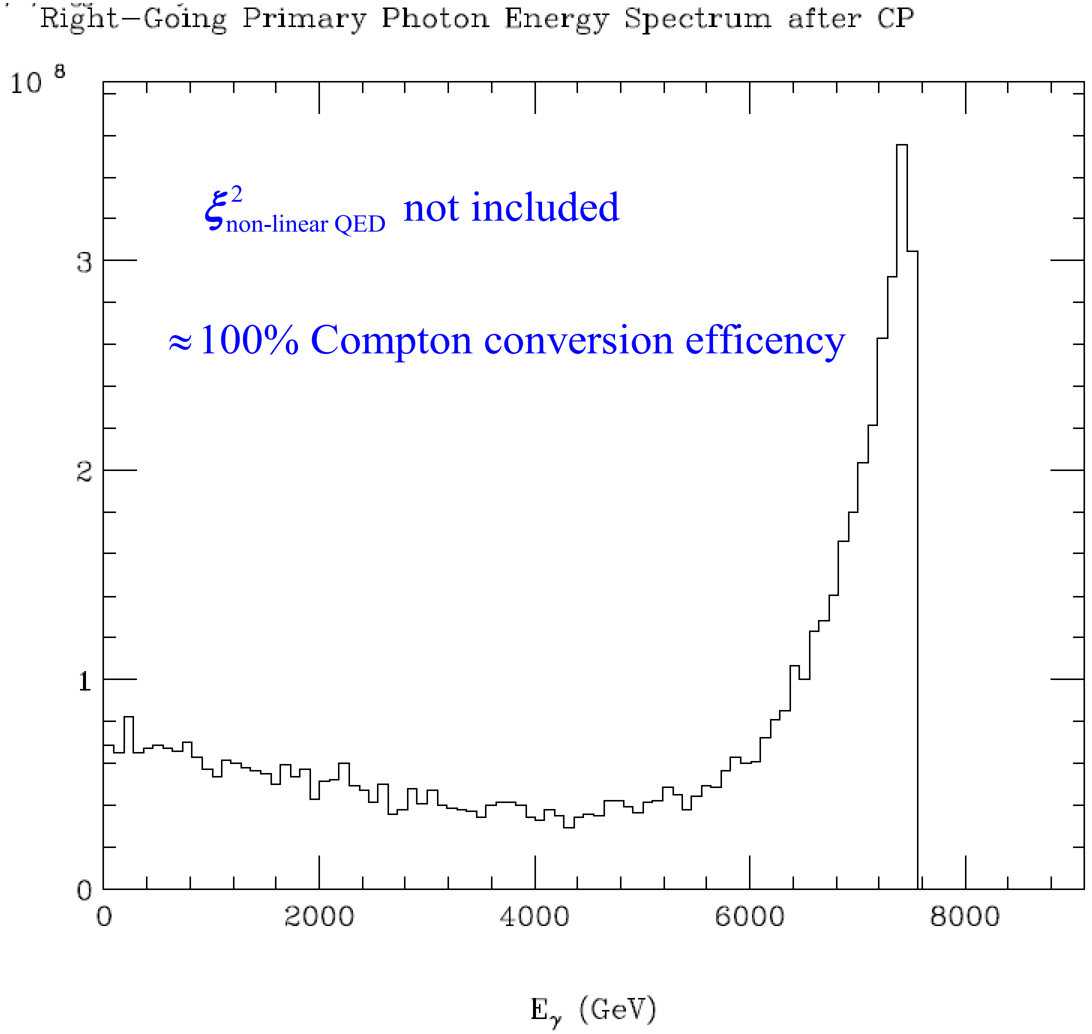

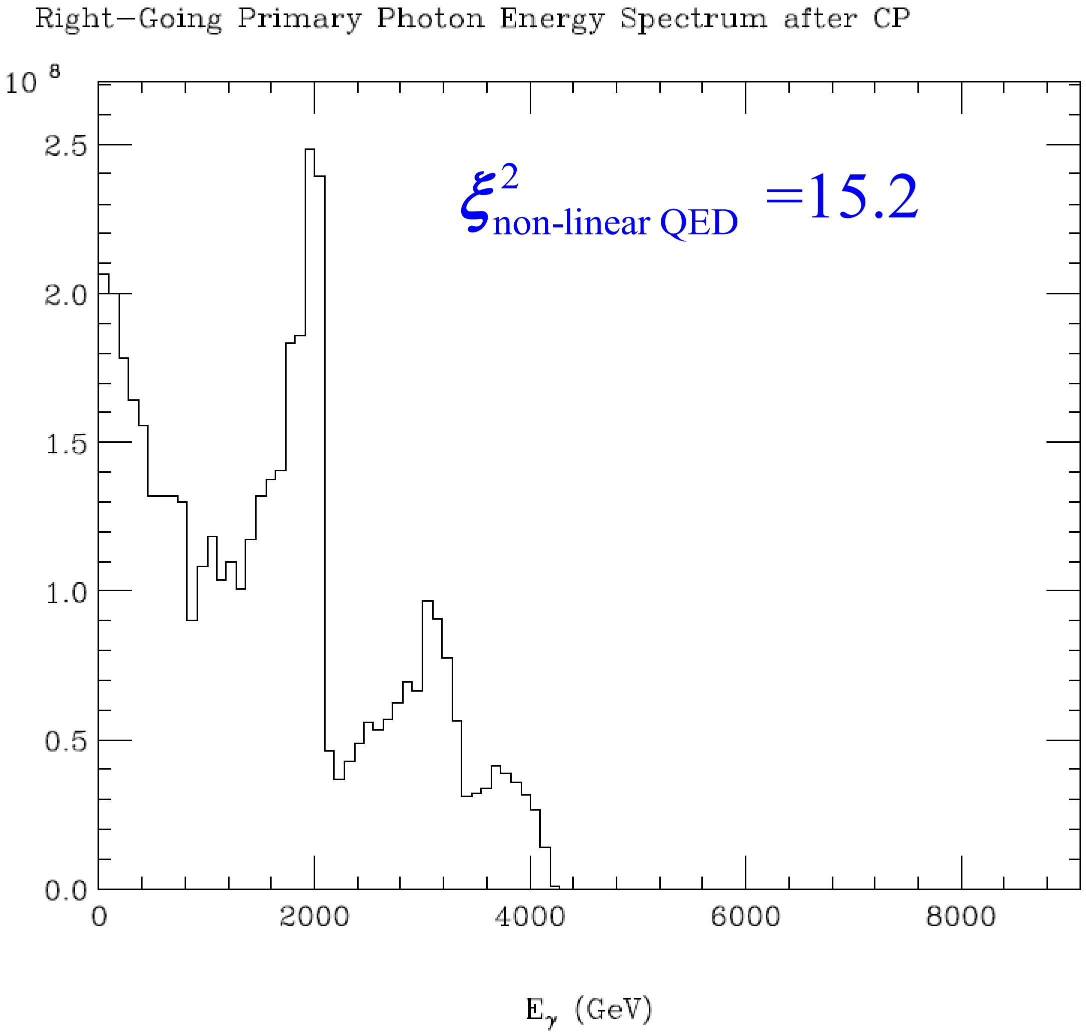

x=4.8 , parameters with ~ 100 % conversion w/ linear QED

$\boldsymbol{x} = 4.8 \;\Rightarrow\; 9100\text{ GeV } \boldsymbol{e}^- + 0.034\text{ eV } \boldsymbol{\gamma}\;\; (\lambda = 36\ \mu\text{m})\quad \boldsymbol{a}_{\gamma FWHM} = 2.1\text{ mm}\quad \boldsymbol{\sigma}_{\gamma z} = 0.79\text{ mm}\quad \text{d}_{\text{cp}} = 2.4\text{ mm}$

$\boldsymbol{\sigma}_{ez} = 5\ \mu\text{m}\quad \text{N}_{e^-} = 1\text{ nC}\quad \gamma\varepsilon_{x,y} = 120\text{ nm}\quad 2\boldsymbol{P}_c\boldsymbol{\lambda}_e = -0.9\qquad \text{E}_{\text{pulse}} = 4400\text{ J}$

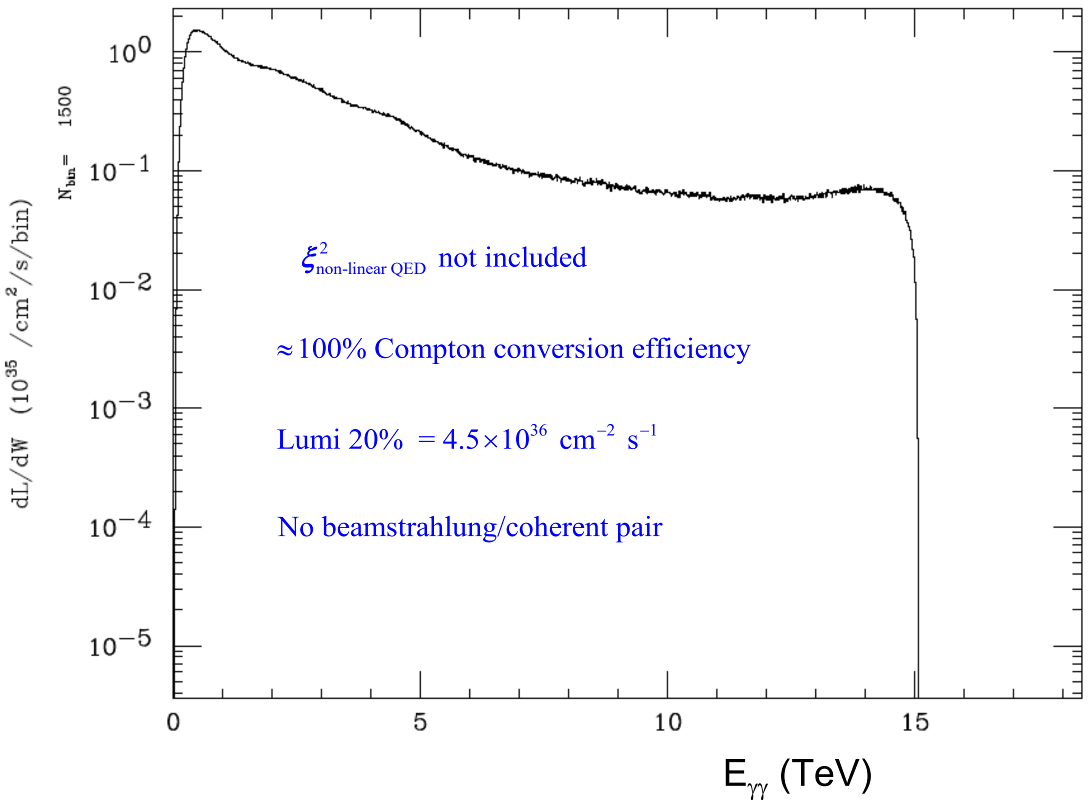

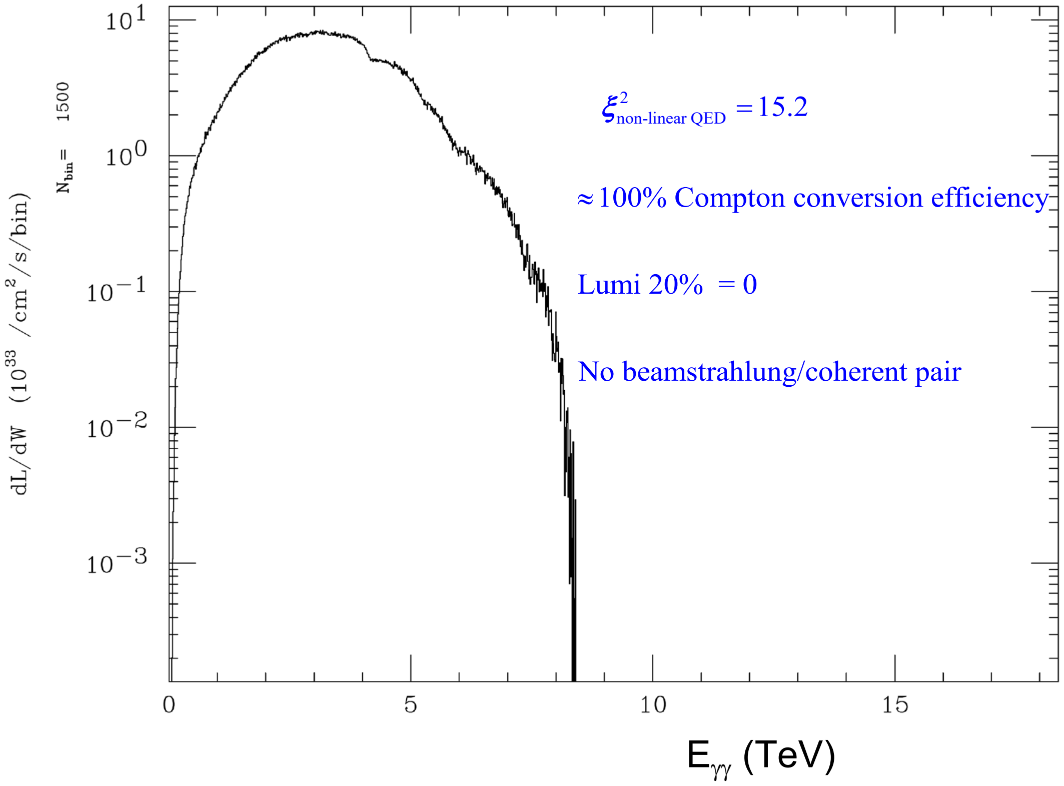

x=4.8 dial back E_{pulse} to get $\xi^2 < 1$

$x = 4.8 \;\Rightarrow\; 9100$ GeV $e^- + 0.034$ eV γ (λ=36 μm) $a_{\gamma FWHM} = 2.1$ mm $\sigma_{\gamma z} = 0.79$ mm $d_{cp} = 2.4$ mm

$\sigma_{ez} = 5\ \mu$m $N_{e^-} = 1$ nC $\gamma\varepsilon_{x,y} = 120$ nm $2P_c\lambda_e = -0.9$ $E_{pulse} = 260$ J

Right−Going Primary Photon Energy Spectrum after CP

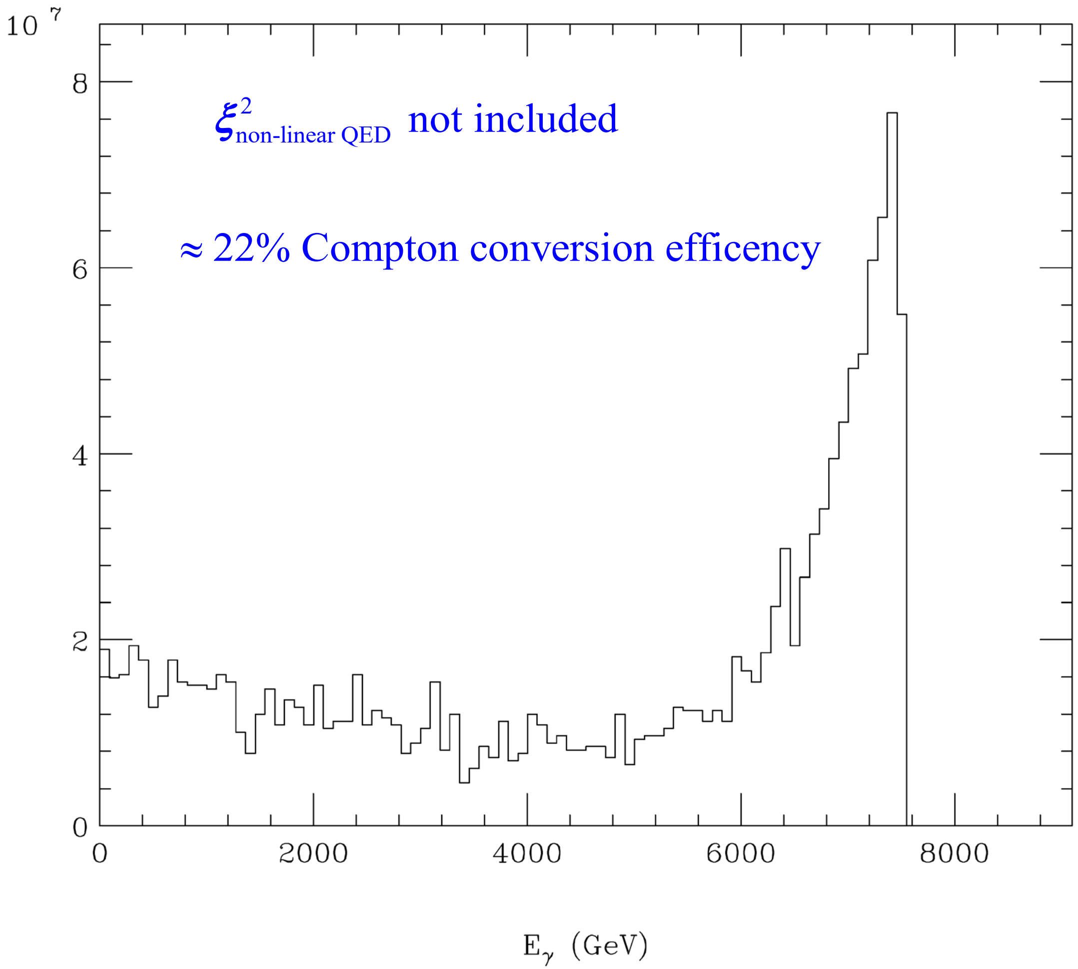

Right−Going Primary Photon Energy Spectrum after CP

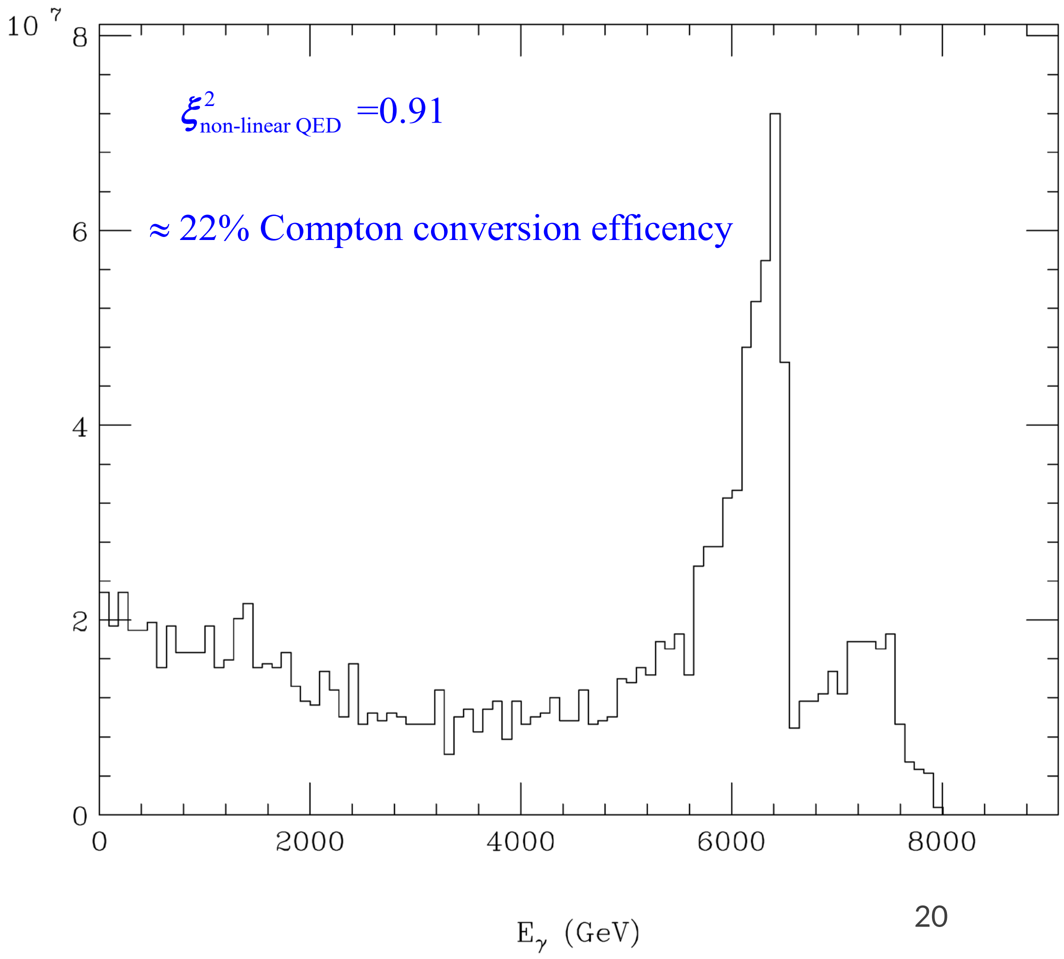

x=4.8 dial back E_{pulse} to get $\xi^2 < 1$

$x = 4.8 \Rightarrow 9100$ GeV $e^- + 0.034$ eV γ (λ=36 μm) $a_{\gamma FWHM} = 2.1$ mm $\sigma_{\gamma z} = 0.79$ mm $d_{cp} = 2.4$ mm

$\sigma_{ez} = 5\ \mu$m N_{e^-} =1 nC $\gamma\varepsilon_{x,y} = 120$ nm $2P_c\lambda_e = -0.9$ $E_{pulse} = 260$ J

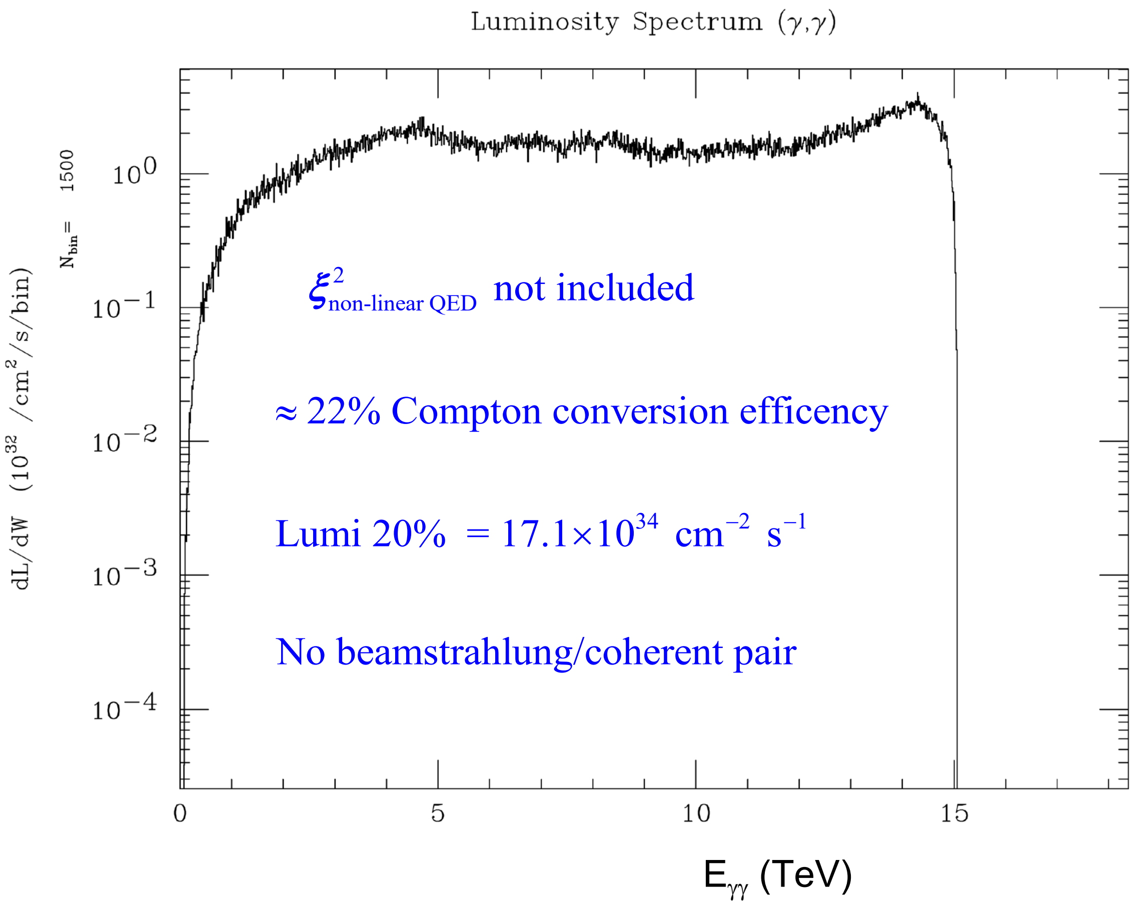

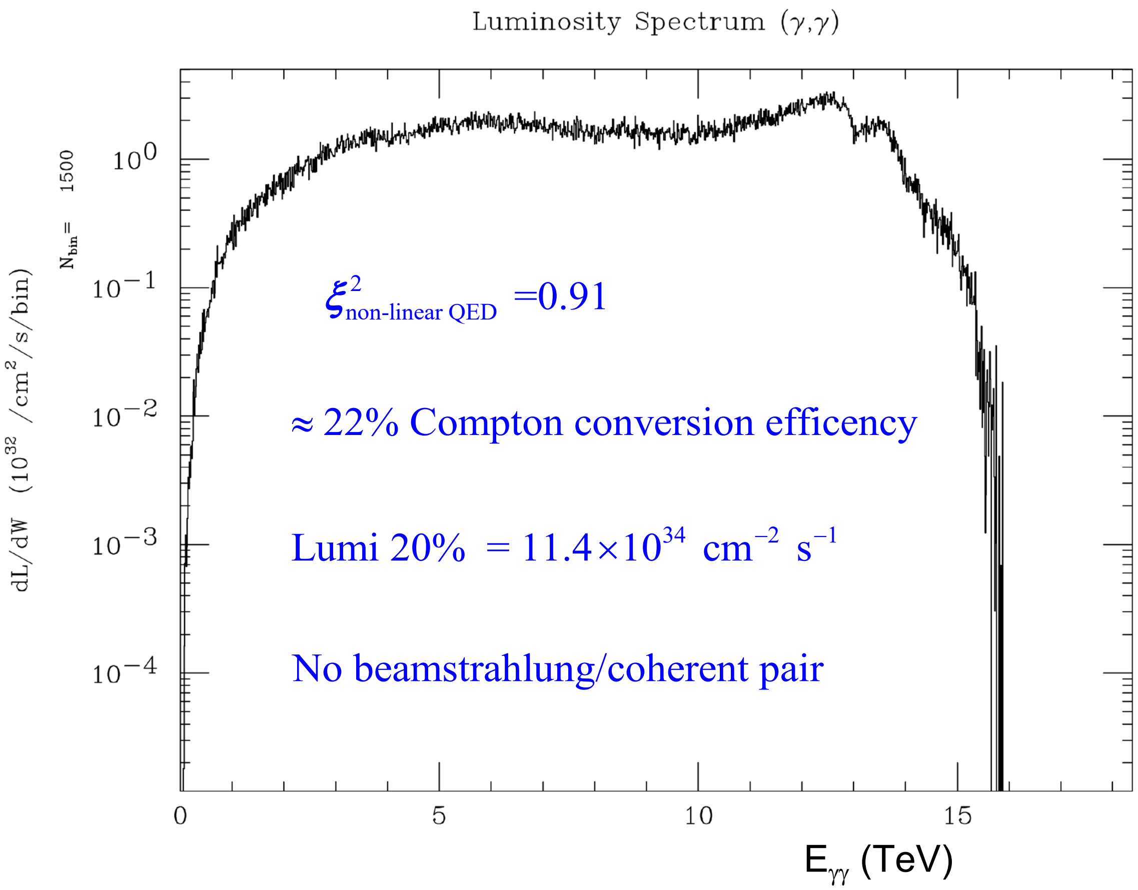

x=40 use spreadsheet bunch charge of $N_e=5\text{x}10^9$

$\boldsymbol{x} = 40 \Rightarrow$ 7875 GeV $\boldsymbol{e}^- +$ 0.33 eV $\boldsymbol{\gamma}$ ($\boldsymbol{\lambda}$=3.7 $\boldsymbol{\mu}$m) $\boldsymbol{a}_{\gamma FWHM} = 0.24$ mm $\boldsymbol{\sigma}_{\gamma z} = 270\ \boldsymbol{\mu}$m $d_{cp} = 0.82$mm

$\boldsymbol{\sigma}_{ez} = 5\ \boldsymbol{\mu}$m $N_{e^-} = 5\times10^9$ $\gamma\varepsilon_{x,y} = 120$ nm $2P_c\lambda_e = -0.9$ $E_{pulse} = 590$ J

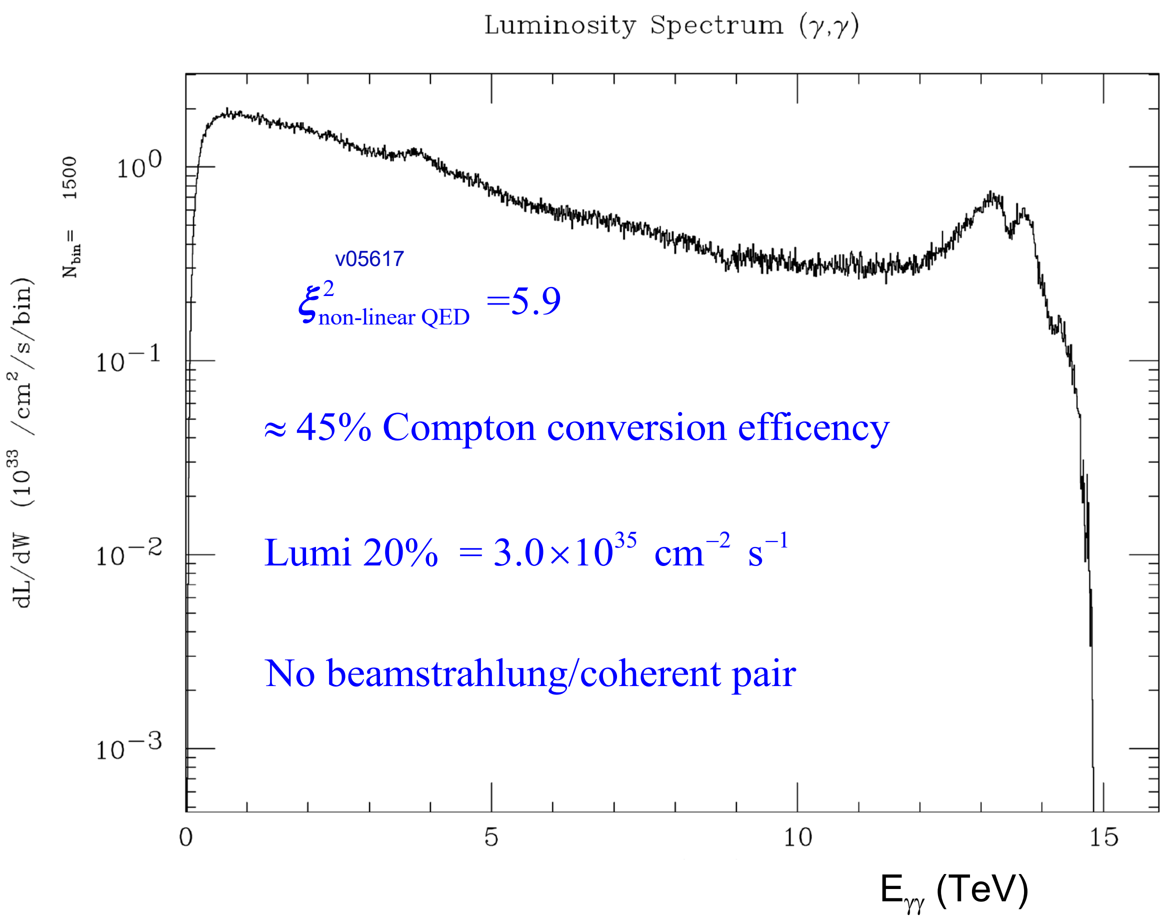

15 TeV and x=40 Turn on coherent processes

$x = 40 \Rightarrow 7875 \text{ GeV } e^- + 0.33 \text{ eV } \gamma \ (\lambda = 3.7\ \mu\text{m})$ $a_{\gamma FWHM} = 0.24$ mm $\sigma_{\gamma z} = 270\ \mu$m $d_{cp} = 0.82$mm

$\sigma_{ez} = 5\ \mu$m $N_{e^-} = 5 \times 10^9$ $\gamma\varepsilon_{x,y} = 120$ nm $2P_c\lambda_e = -0.9$ $E_{pulse} = 590$ J

Halfway through the collision CAIN complains:

(SUBR.COHPAR) Algorithm of coherent pair generation wrong.
Call the programmer prob,pmaxco= 8.309E-01 8.000E-01

Solution:

number of macro particles produced per coherent beamstrahlung photon = 1 → 0.01
number of pairs of macro particles produced per coherent e+e- pair = 1 → 0.0001
number of macro particles produced per incoherent particle = 1 → 0.01

15 TeV and x=40 Turn on coherent processes

$x = 40 \Rightarrow$ 7875 GeV $e^- +$ 0.33 eV γ (λ=3.7 μm) $a_{\gamma FWHM} = 0.24$ mm $\sigma_{\gamma z} = 270\ \mu$m $d_{cp} = 0.82$mm

$\sigma_{ez} = 5\ \mu$m $N_{e^-} = 5\times10^9$ $\gamma\varepsilon_{x,y} = 120$ nm $2P_c\lambda_e = -0.9$ $E_{pulse} = 590$ J

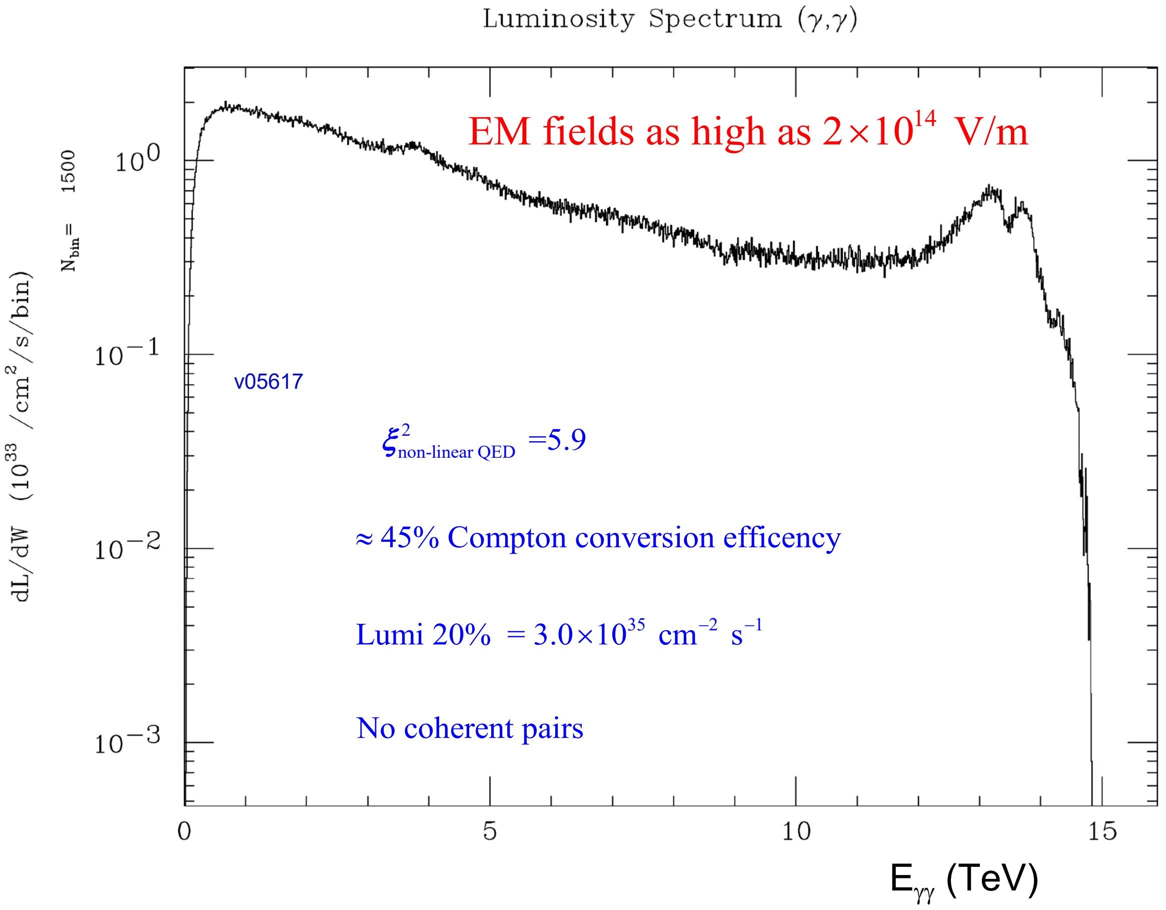

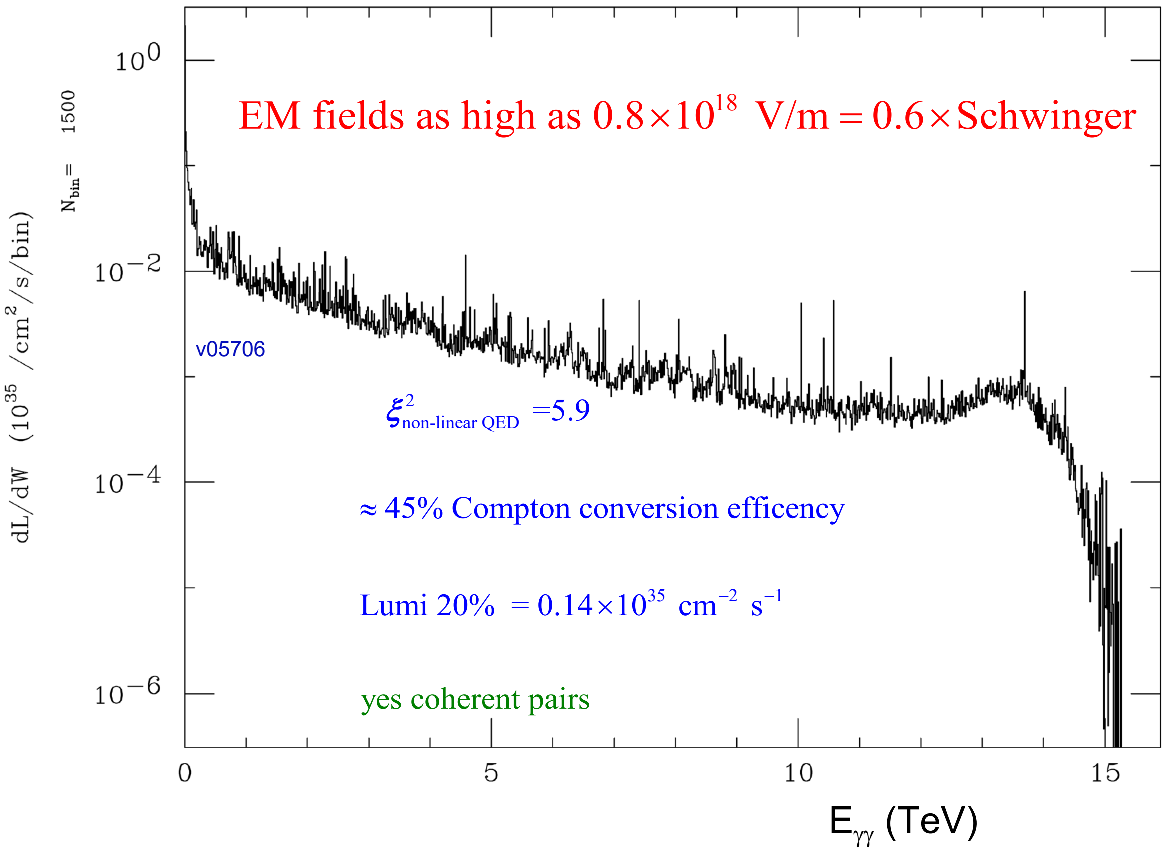

Coherent pair production eats up the 7.5 TeV photons and produces many e+ that pinch the e- beam leading to higher fields and even more coherent pair production.

$e^- \gamma$ collisions at $E_{e\gamma}$=140 GeV I.P. geometric e^- σ_x,σ_y=5.1 nm

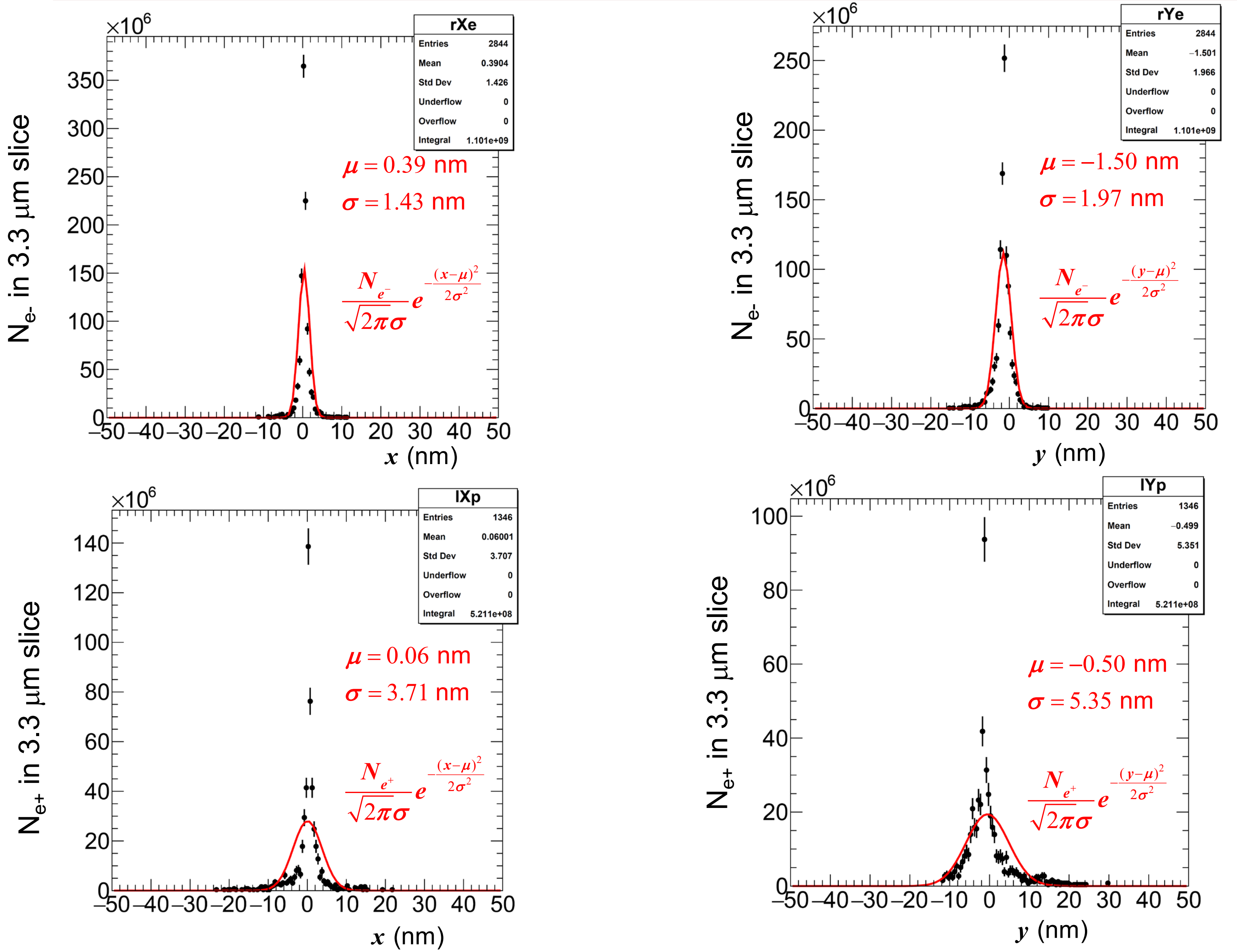

During the collision, the e^+ from coherent e^+e^- production are focused by the EM field of the oncoming e^- beam. This leads to focusing (pinching) of the e^- beam.

This pinching creates very high fields which leads to even more coherent pair production and even higher fields.

x=1.2x10^5 (1 keV γ) not affected as much by coherent processes

$x = 1.2\times10^{5} \;\Rightarrow\; 7500$ GeV e^{-} + 1 keV γ (λ=1.2 nm)

$a_{\gamma FWHM} = 70$ mm $\quad \sigma_{\gamma z} = 5\ \mu$m $\quad d_{cp} = 15\ \mu$m

$\sigma_{ez} = 5\ \mu$m $\quad N_{e^-} = 6\times10^{9} \quad \gamma\varepsilon_{x,y} = 120$ nm

$2P_c\lambda_e = +0.9 \quad E_{pulse} = 0.72$ J

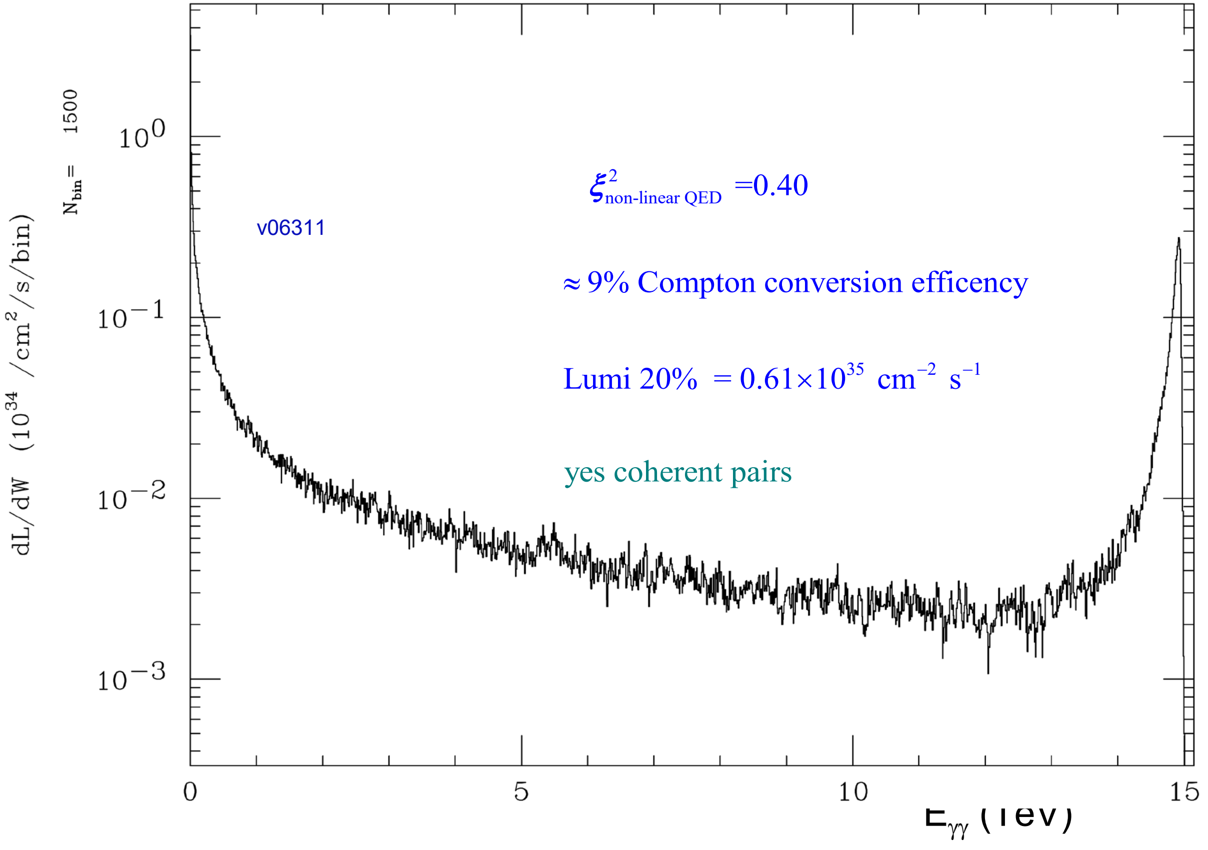

$x = 40 \;\Rightarrow\; 7875$ GeV e^{-} + 0.33 eV γ (λ=3.7 μm)

$a_{\gamma FWHM} = 0.24$ mm $\quad \sigma_{\gamma z} = 270\ \mu$m $\quad d_{cp} = 0.82$mm

$\sigma_{ez} = 5\ \mu$m $\quad N_{e^-} = 5\times10^{9} \quad \gamma\varepsilon_{x,y} = 120$ nm

$2P_c\lambda_e = -0.9 \quad E_{pulse} = 590$ J

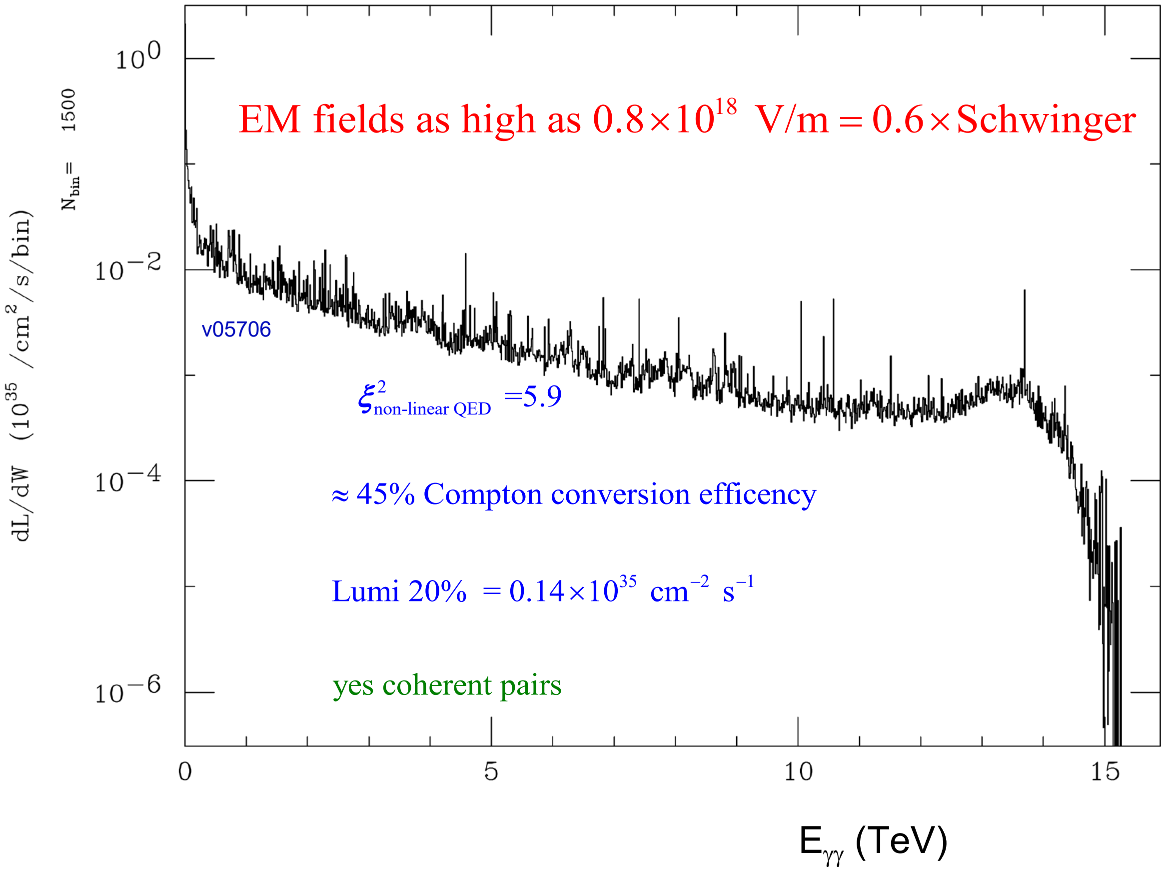

15 TeV $x=1.2\text{x}10^5$ vs $x=40$

$x = 1.2\times10^5 \Rightarrow$ 7500 GeV $e^- +$ 1 keV γ (λ=1.2 nm)

$a_{\gamma FWHM} = 70$ mm $\sigma_{\gamma z} = 5\ \mu$m $d_{cp} = 15\ \mu$m

$\sigma_{ez} = 5\ \mu$m $N_{e^-} = 6\times10^9$ $\gamma\varepsilon_{x,y} = 120$ nm

$2P_c\lambda_e = +0.9$ $E_{pulse} = 0.72$ J

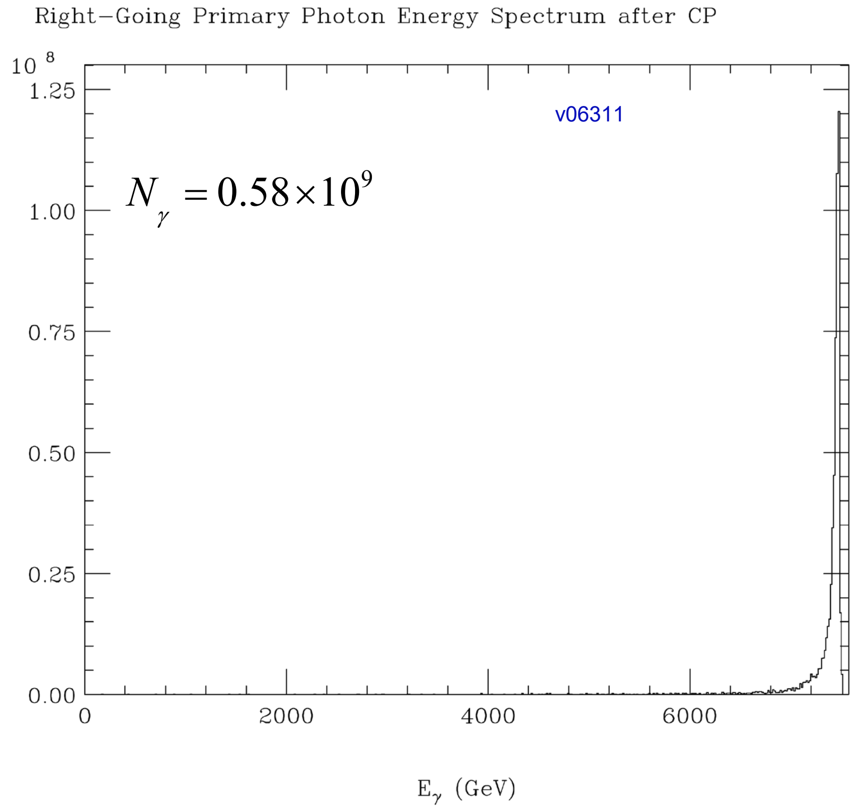

$x = 40 \Rightarrow$ 7875 GeV $e^- +$ 0.33 eV γ (λ=3.7 μm)

$a_{\gamma FWHM} = 0.24$ mm $\sigma_{\gamma z} = 270\ \mu$m $d_{cp} = 0.82$mm

$\sigma_{ez} = 5\ \mu$m $N_{e^-} = 5\times10^9$ $\gamma\varepsilon_{x,y} = 120$ nm

$2P_c\lambda_e = -0.9$ $E_{pulse} = 590$ J

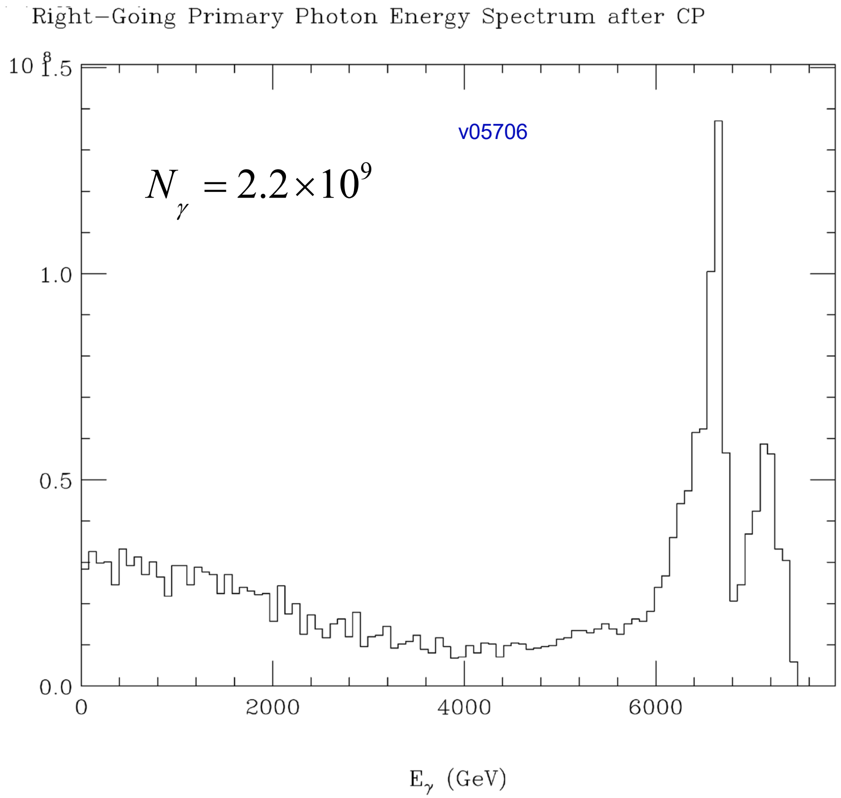

15 TeV x=1.2x10^5 vs x=40

$x = 1.2\times10^5 \Rightarrow$ 7500 GeV $e^- +$ 1 keV γ (λ=1.2 nm)

$a_{\gamma FWHM} = 70$ mm $\sigma_{\gamma z} = 5\ \mu$m $d_{cp} = 15\ \mu$m

$\sigma_{ez} = 5\ \mu$m $N_{e^-} = 6\times10^9$ $\gamma\varepsilon_{x,y} = 120$ nm

$2P_c\lambda_e = +0.9$ $E_{pulse} = 0.72$ J

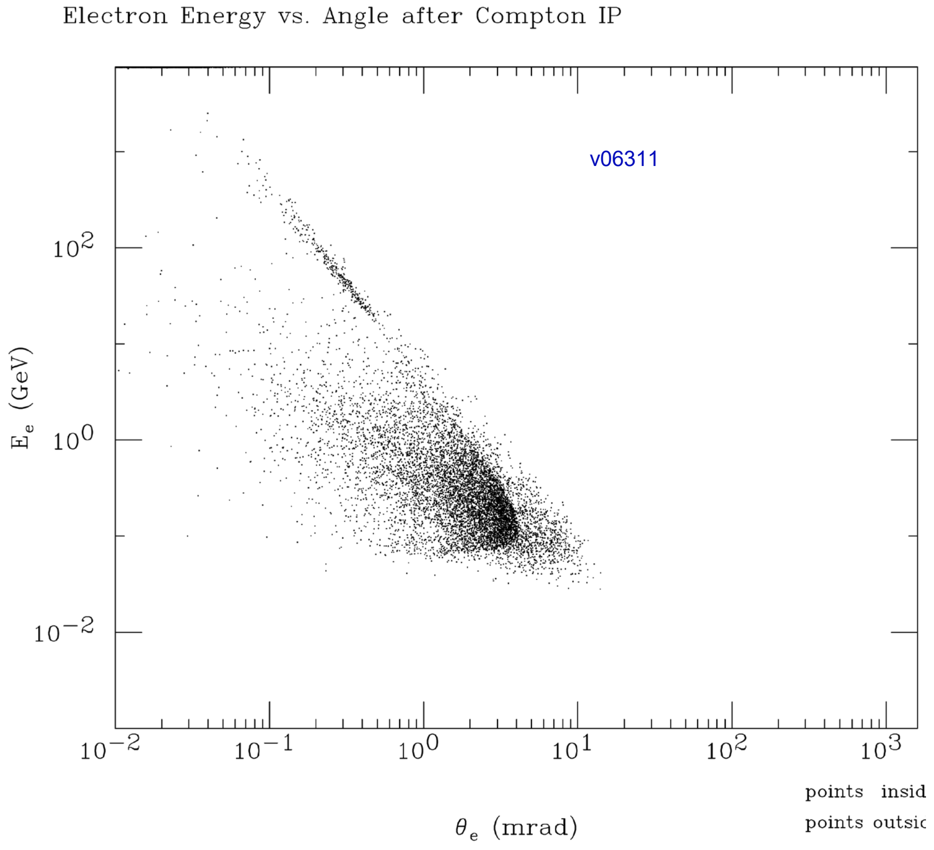

$x = 40 \Rightarrow$ 7875 GeV $e^- +$ 0.33 eV γ (λ=3.7 μm)

$a_{\gamma FWHM} = 0.24$ mm $\sigma_{\gamma z} = 270\ \mu$m $d_{cp} = 0.82$mm

$\sigma_{ez} = 5\ \mu$m $N_{e^-} = 5\times10^9$ $\gamma\varepsilon_{x,y} = 120$ nm

$2P_c\lambda_e = -0.9$ $E_{pulse} = 590$ J

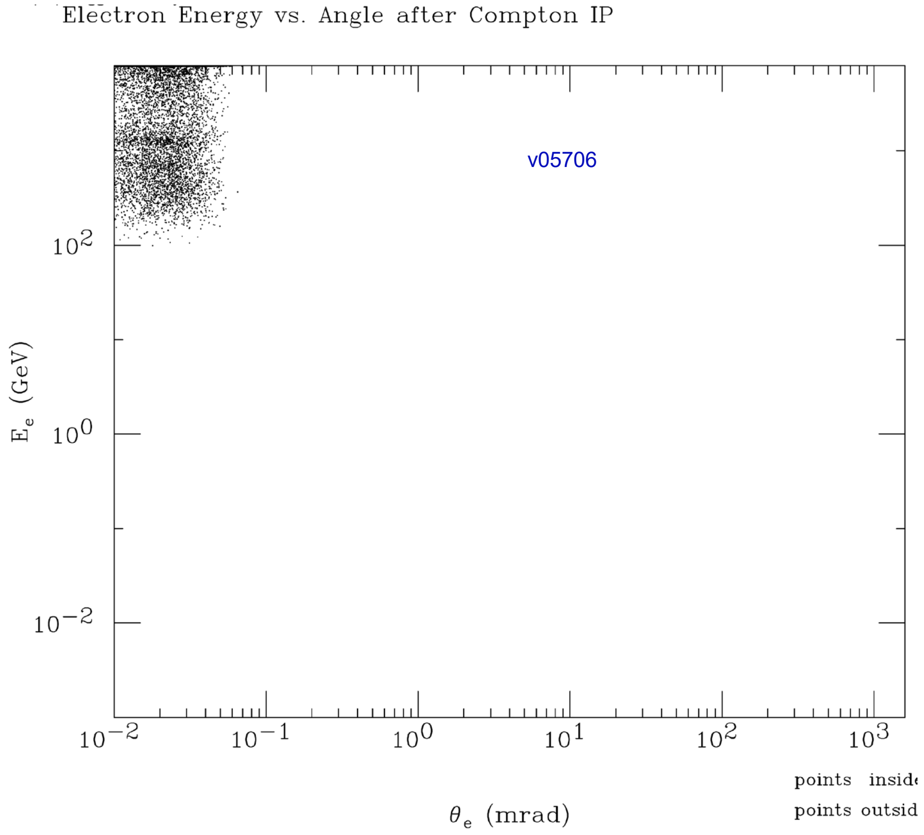

x=1.2 x 10^5 calculation, however, is missing an important piece

$x = 1.2\times10^5 \Rightarrow 7500\ \text{GeV}\ e^- + 1\ \text{keV}\ \gamma\ (\lambda = 1.2\ \text{nm})$ $a_{\gamma FWHM} = 70\ \text{mm}$ $\sigma_{\gamma z} = 5\ \mu\text{m}$ $d_{cp} = 15\ \mu\text{m}$

$\sigma_{ez} = 5\ \mu\text{m}$ $N_{e^-} = 1\ \text{nC}$ $\gamma\varepsilon_{x,y} = 120\ \text{nm}$ $2P_c\lambda_e = +0.9$ $E_{pulse} = 0.72\ \text{J}$

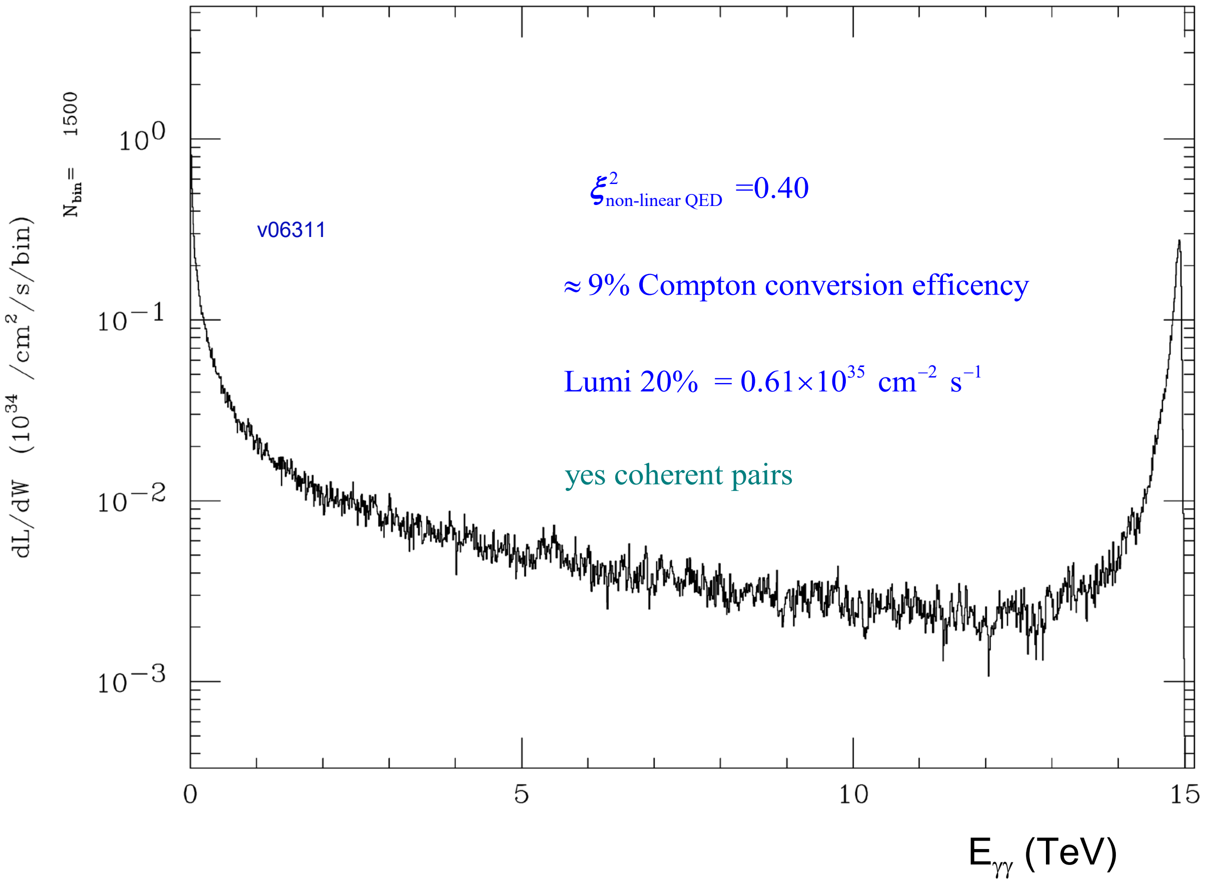

$\gamma\gamma \to N\times e^+e^-$, $e^-\gamma \to e^- + N\times e^+e^-$, $N = 2,3,\ldots$ are not simulated by CAIN. These processes can be ignored for $x \le 1000$, but not for $x = 1.2\times10^5$

x	$\frac{\sqrt{s_{e^-\gamma}}}{m_e} = \sqrt{x+1}$	$\frac{\sqrt{s_{e^-\gamma}}}{m_e} m_W$ (TeV)
4.82	2.4	0.2
1000	32	2.5
1.2×10^5	350	28

Ignoring these processes would be the equivalent of ignoring multiple 4,5,... W boson production in e^+e^- or $\gamma\gamma$ collisions. This is OK at 0.2 TeV & 2.5 TeV due to phase space suppression, but not OK at 28 TeV.

15 TeV $\gamma\gamma$ Collider Simulation Summary

- Not surprisingly, it is not straightforward to extrapolate a Compton $\sqrt{s} = 125$ GeV $\gamma\gamma$ collider to 15 TeV
- A value of $x = 4.8$ requires e^-e^- Ecm=9100 GeV for Ecm=7500 GeV $\gamma\gamma$ and has very broad lumi spectrum
- A value $x = 40$ requires e^-e^- Ecm=7800 GeV for Ecm=7500 GeV $\gamma\gamma$. But when coherent processes are considered, EM fields produced by the tightly focused e^- beams lead to significant coherent beamstrahlung and e^+e^- pair-production for moderate values of x This is excaberated by the produced e^+ which pinch the e^- beams leading to even higher EM fields. These effects serve to diminish the $\gamma\gamma$ luminosity in the top 20% of the $\sqrt{\hat{s}}$ distribution.
- A multi-TeV $\gamma\gamma$ collider with extremely large values of $x \approx 10^5$, corresponding to soft x-ray Compton scattering, does not suffer as much from coherent processes, gives a top 20% luminosity as large as an $x = 40$ $\gamma\gamma$ collider, and has an XCC-like luminosity spectrum with a relatively narrow peak near the maximum center-of-mass energy
- But, $\gamma\gamma \to N\times\ e^+e^-$, $e^-\gamma \to e^- + N\times\ e^+e^-$, $N = 2, 3, \ldots$ are important for $x \approx 10^5$ and must be included in beam-beam simulations to properly evaluate a 15 TeV $\gamma\gamma$ collider with $x \approx 10^5$

Backup

XCC: XFEL Compton $\gamma\gamma$ Collider Higgs Factory

XCC s-channel $\gamma\gamma \to H$ @ $\sqrt{s} = 125$ GeV

$\gamma\gamma \to HH$ @ $\sqrt{s} = 380$ GeV

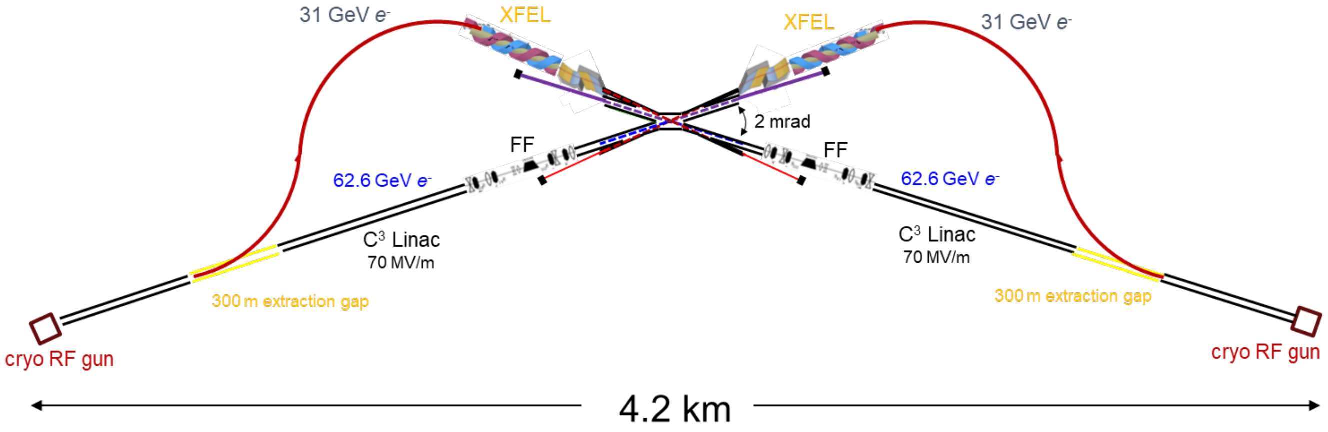

Final Focus parameters	Approx. value	XFEL parameters	Approx. value
Electron energy	62.8 GeV	Electron energy	31 GeV
Electron beam power	0.57 MW	Electron beam power	0.28 MW
β_x/β_y	0.03/0.03 mm	normalized emittance	120 nm
$\gamma\epsilon_x/\gamma\epsilon_y$	120/120 nm	RMS energy spread $\langle\Delta\gamma/\gamma\rangle$	0.05%
σ_x/σ_y at e^-e^- IP	5.4/5.4 nm	bunch charge	1 nC
σ_z	20 μm	Linac-to-XFEL curvature radius	133 km
bunch charge	1 nC	Undulator B field	$\gtrsim 1$ T
Rep. Rate at IP	240 × 38 Hz	Undulator period λ_u	9 cm
σ_x/σ_y at IPC	12.1/12.12 nm	Average β function	12 m
$\mathcal{L}_{\text{geometric}}$	9.7×10^{34} cm^2 s^{-1}	x-ray λ (energy)	1.2 nm (1 keV)
δ_E/E	0.05%	x-ray pulse energy	0.7 J
L^* (QD0 exit to e^- IP)	1.5m	pulse length	40 μm
d_{cp} (IPC to IP)	60 μm	$a_{\gamma x}/a_{\gamma y}$ (x/y waist)	21.2/21.2 nm
QD0 aperture	9 cm diameter	non-linear QED ξ^2	0.10
Site parameters	Approx. value		
crossing angle	2 mrad		
total site power	85 MW		
total length	3.0 km		

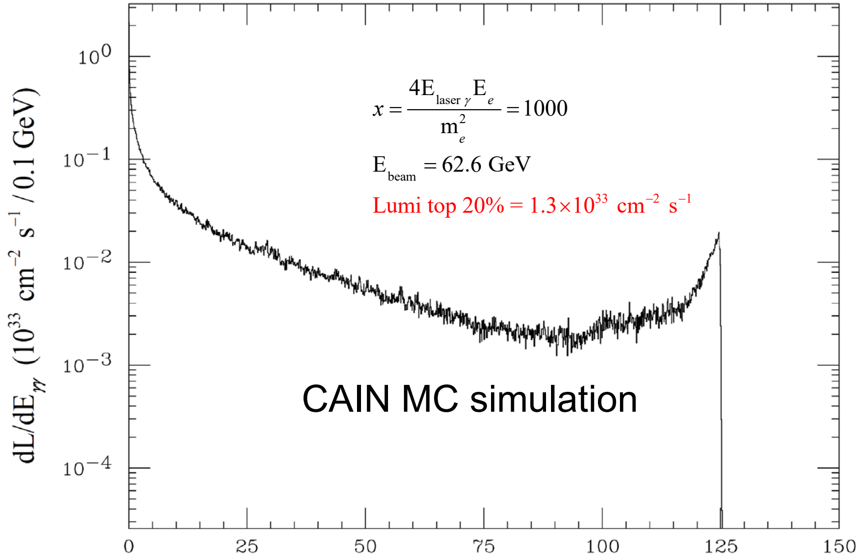

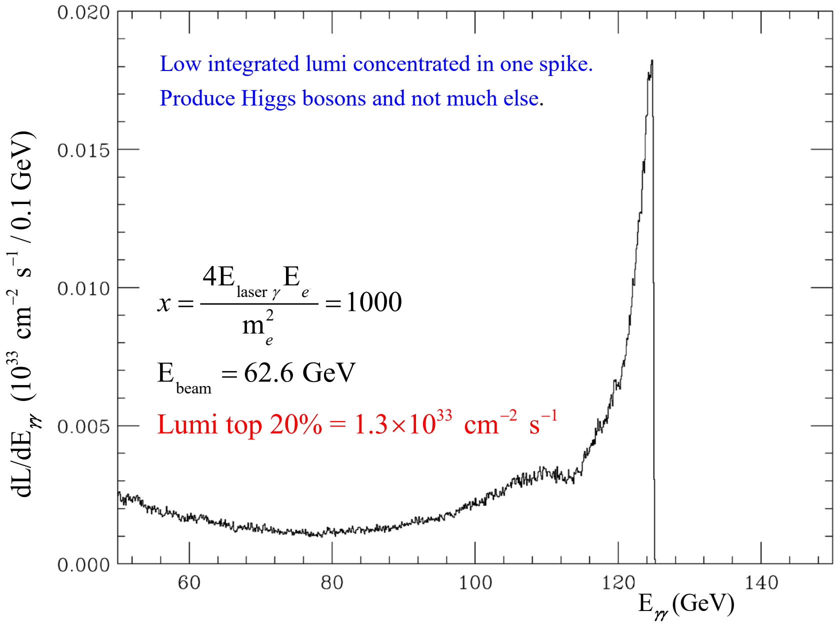

Does CAIN Simulate the Field of Coherent e^+e^- Pairs ?

- In recent private communication with Spencer, CAIN author K. Yokoya says NO.

- CAIN manual is silent on the issue w.r.t. coherent pairs, but does mention incoherent pairs:

> Particles created by incoherent processes do not contribute in creating the beam field. Also note that the parent macro-particles do not change by particle-particle interaction. All these come from the actual situation in linear colliders where the incoherent particles are much less in number compared with the initial particles.

- In the FORTRAN code, incoherently produced particles are given names such as 'IBW ', 'IBH ', 'ILL ' , 'IBR ' , whereas all other particles -- including coherently produced e^+e^- -- are given 4 spaces: '   '.

- The FORTAN code that calculates the EM field is filled with loops like this

```
DO 300 N=1,NP
      IF(ISBIN(N).NE.IS) GOTO 300
      IF(KIND(N).EQ.1) GOTO 300
      IF(LOST(N).NE.0) GOTO 300
      IF(PNAME(N).NE.'    ') GOTO 300
      IF(TXYS(0,N).GT.T) GOTO 300
```

Replace CAIN EM FFT EM Field Calculation with Bassetti-Erskine 2d Gaussian Expression

Bassetti-Erskine

$(0,0) =$ center of charge distribution

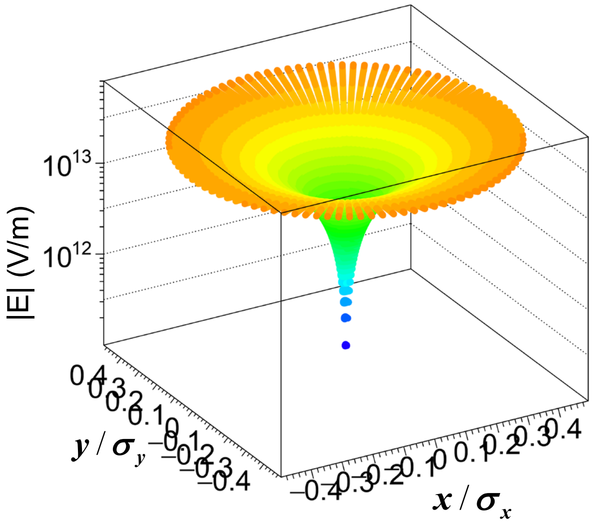

CAIN

$(0,0) =$ center of charge distribution

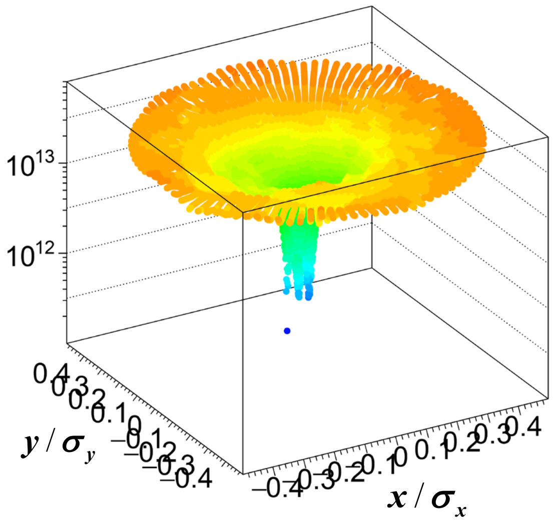

CAIN

$(0,0) =$ EM field minimum

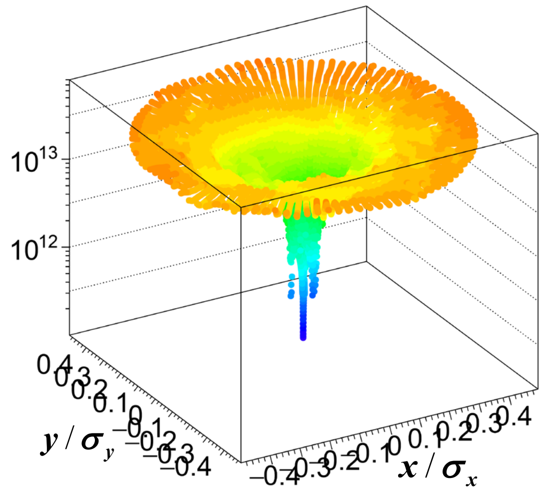

Replace CAIN EM FFT EM Field Calculation with Bassetti-Erskine 2d Gaussian Expression

Bassetti-Erskine 1 Gaussian

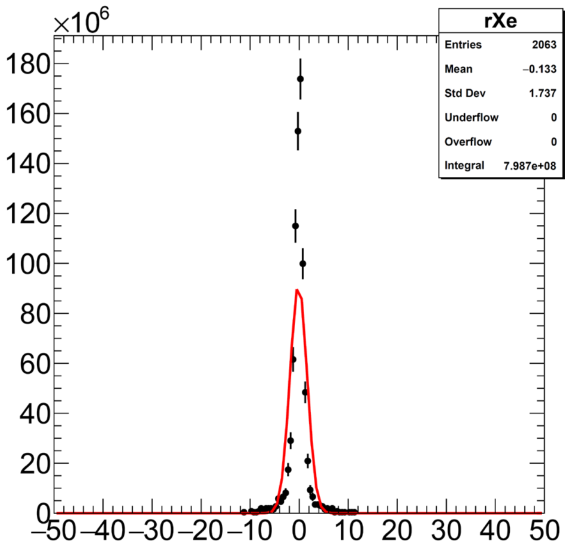

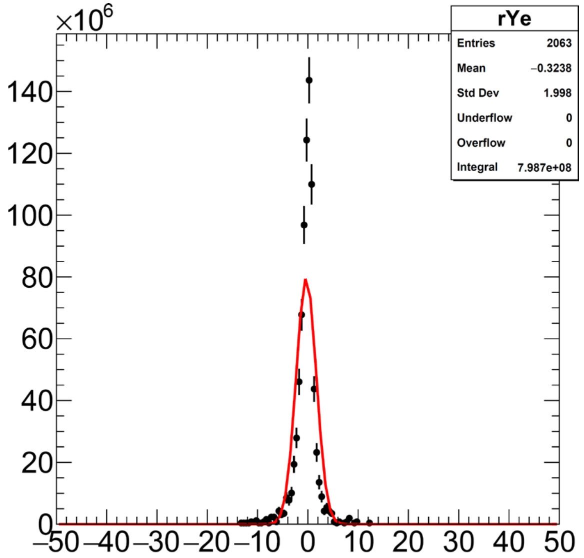

Bassetti-Erskine 2 Gaussians

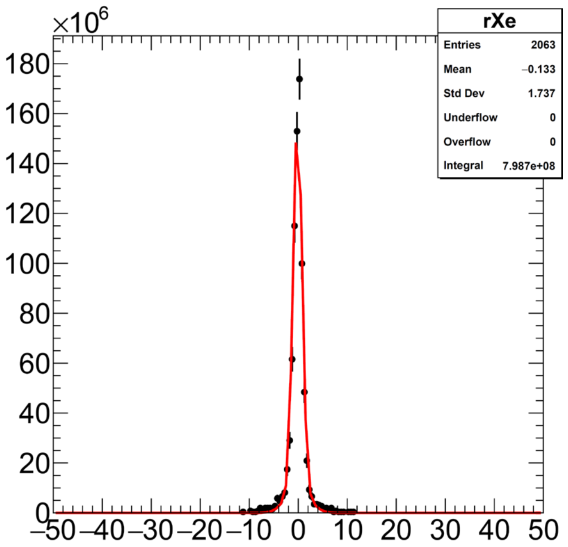

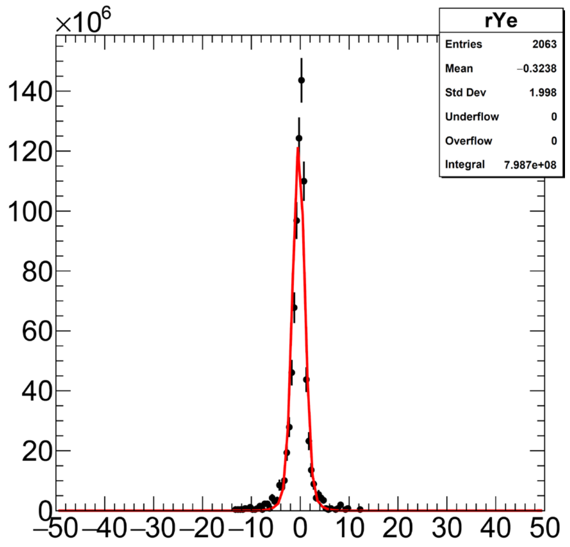

Replace CAIN EM FFT EM Field Calculation with Bassetti-Erskine 2d Gaussian Expression

Bassetti-Erskine 1 Gaussian vs Bassetti-Erskine 2 Gaussian for γγ collision

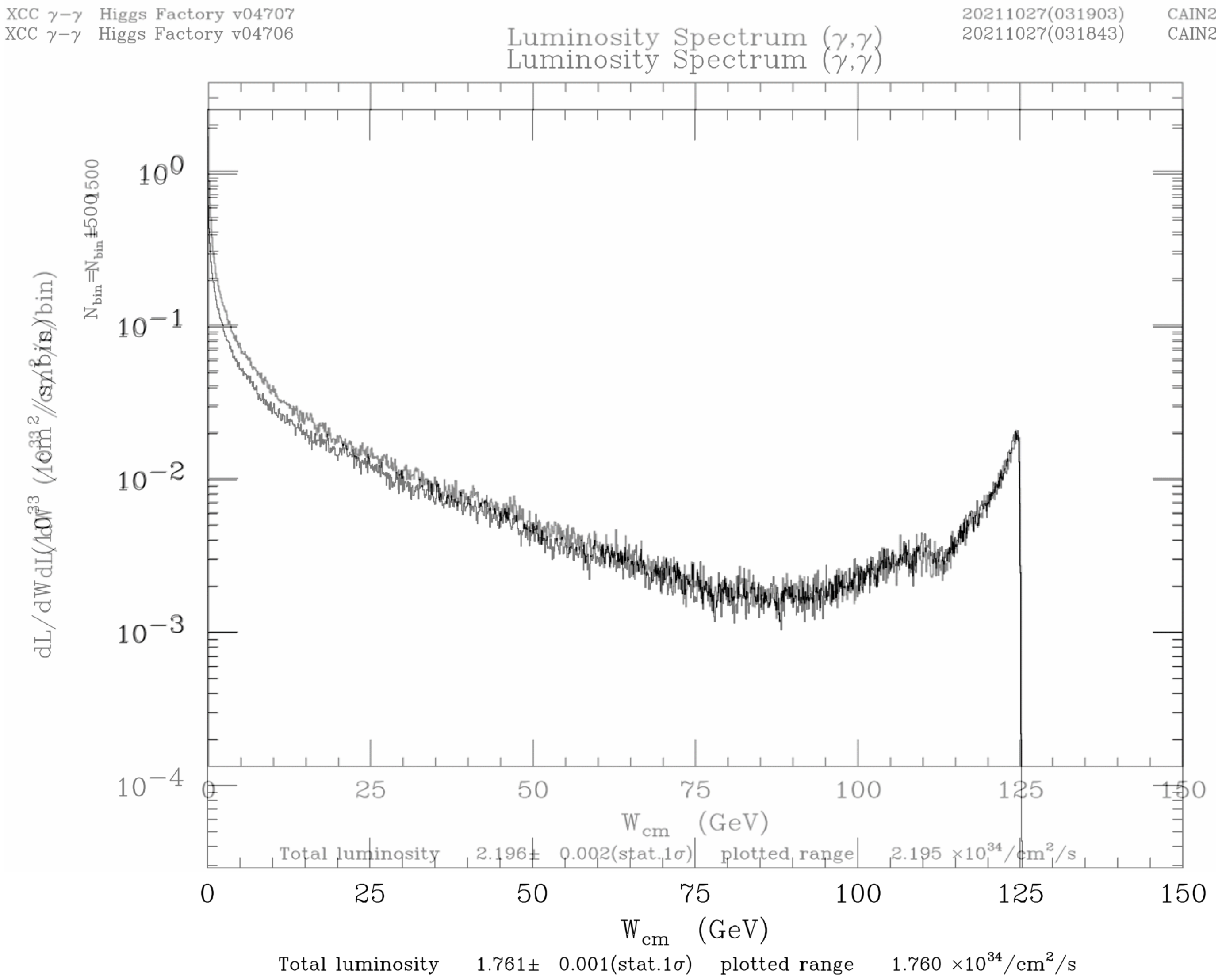

Replace CAIN EM FFT EM Field Calculation with Bassetti-Erskine 2d Gaussian Expression

2 Gaussian Bassetti-Erskine vs CAIN EM Field

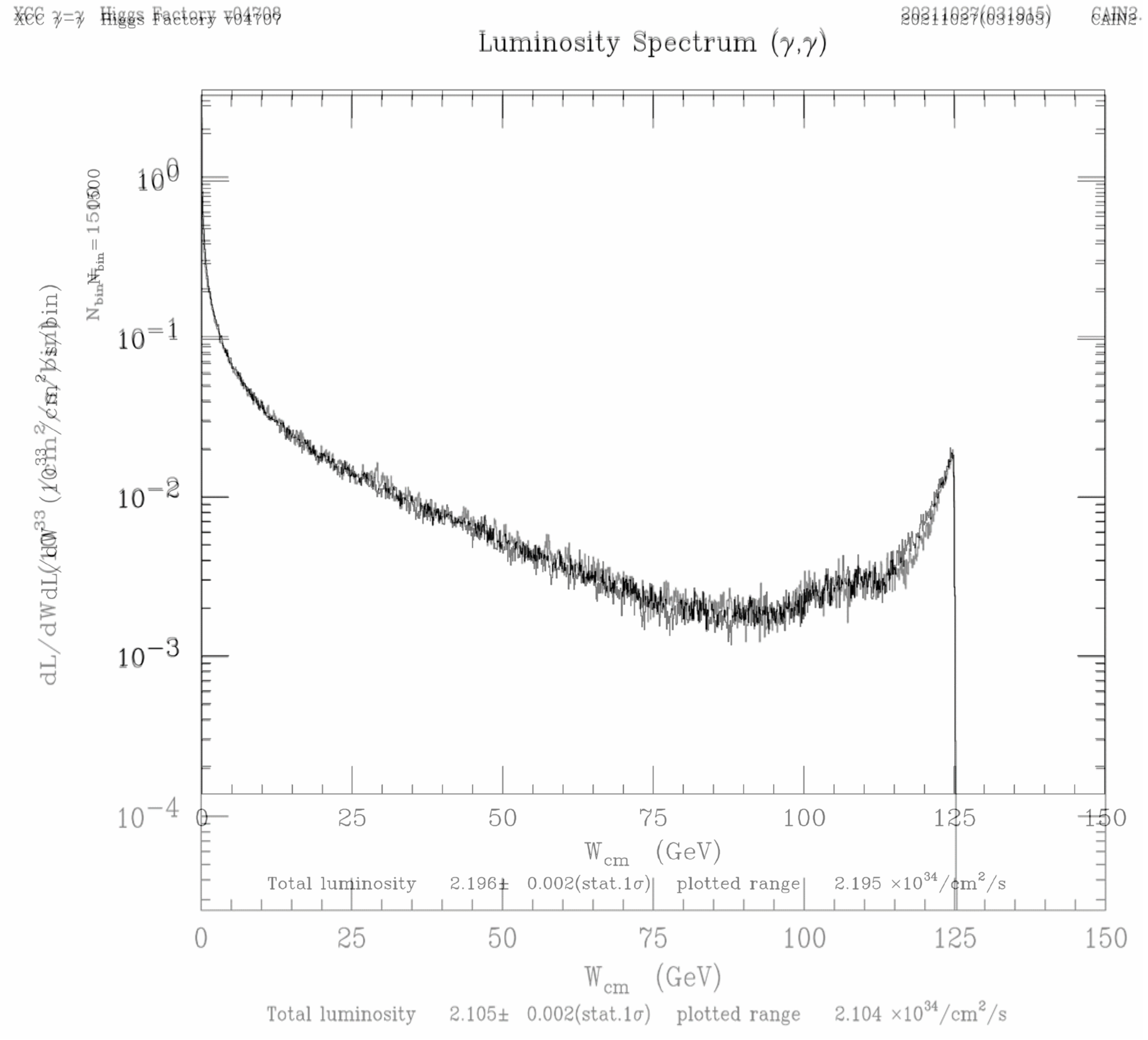

Wenlong Zhang Also Sees Pinching in e⁻e⁻ Collisions

Luminosity: decreased by the disruption

Wenlong Zhang

TÉCNICO LISBOA

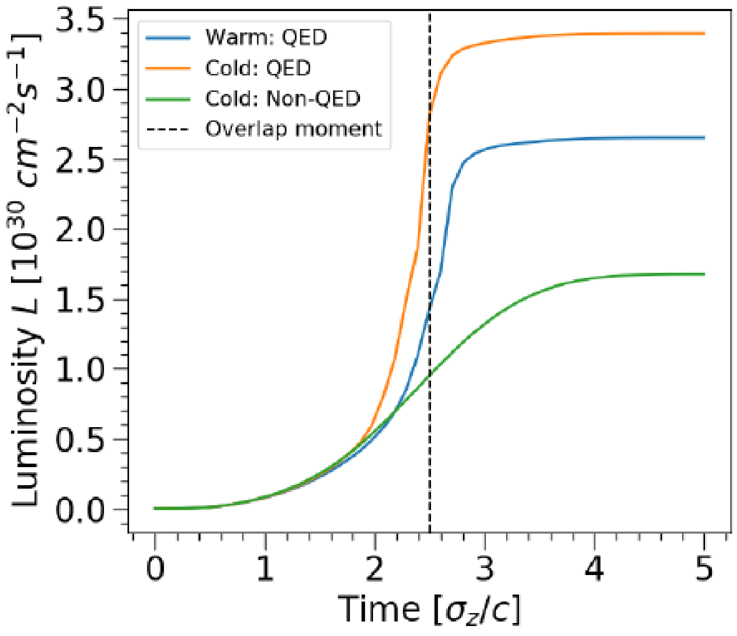

Luminosity:

- Warm beams: $L = 2.65 \times 10^{30}\ cm^{-2}s^{-1}$
- Cold beams: $L = 3.39 \times 10^{30}\ cm^{-2}s^{-1}$
- Non-QED simulation with cold beams: $L = 1.68 \times 10^{30}\ cm^{-2}s^{-1}$

Geometric luminosity:

$$L_0 = \frac{N_0^2}{4\pi\sigma_0^2}$$

$$= 1.18 \times 10^{31}\ cm^{-2}s^{-1}$$

Conclusions:

- Because the beams are expelled away from each other, the luminosity is smaller than the geometry luminosity L_0
- The density pinch, shown before, leads to the luminosity enhancement, compared with the non-QED simulation where the density pinch doesn't occur.

Machine Detector Interface at XCC

Backgrounds from e^+, e^-, γ produced at Compton IP's and primary IP:

(1) Vertex detector inner radius (incoherent e^+e^- pairs from primary IP - same situation as e^+e^- linear colliders)

(2) Beampipe X_0 (moderate soft X-ray flux from Compton IP's $|\cos\theta| < 0.95$)

(3) Forward boundaries of the main tracker/calorimeter and solid angle coverage of forward detector (large hard X-ray flux from Compton IP's $|\cos\theta| > 0.95$)

(4) Aperture of final quad (e^+, e^-, γ from primary & Compton IP's must pass through this aperture)

Vertex Detector Inner Radius

CAIN Simulation assuming 5 T Solenoid

$E(e^{\pm})$ vs. R at $z = 6.25$ cm

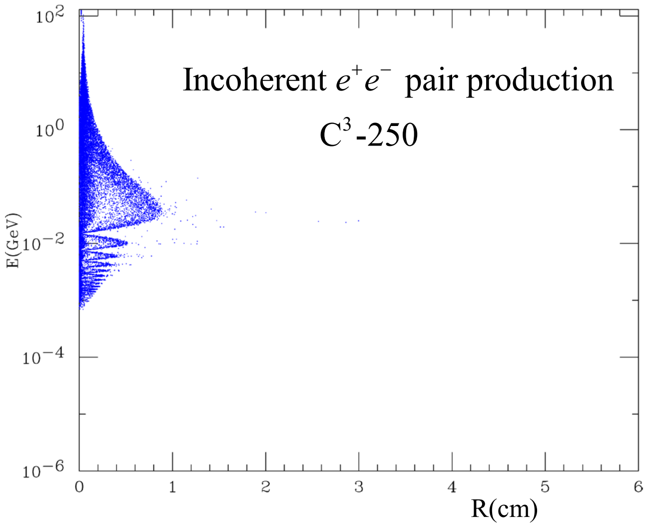

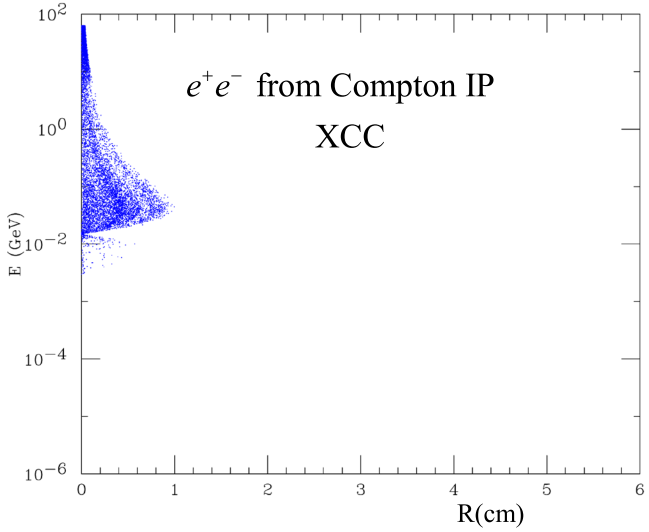

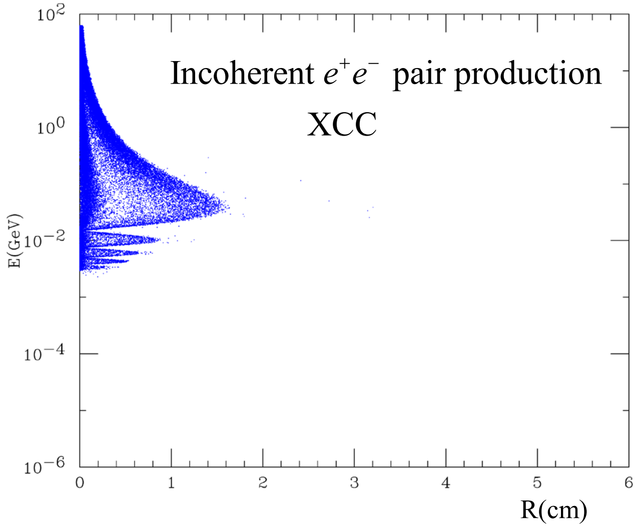

$N(e^{\pm})$ vs. R at $z = 6.25$ cm

SiD Vtx Inner Rad=1.5 cm

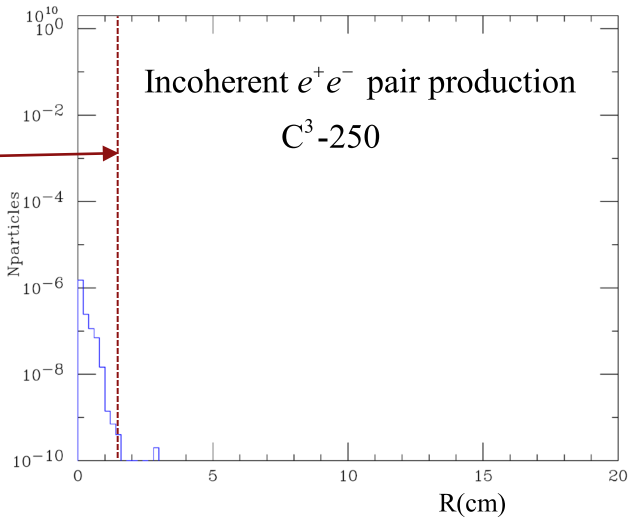

XCC Vtx Inner Rad=1.9 cm should be OK

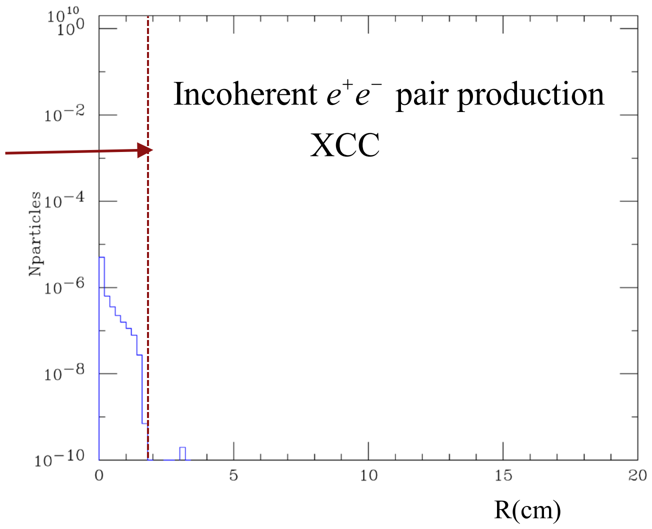

X-rays from Compton IP's

CAIN Simulation

Moderate flux of soft (few keV) X-rays in central region

Number and energy of Compton IP X-rays increases rapidly in the forward region

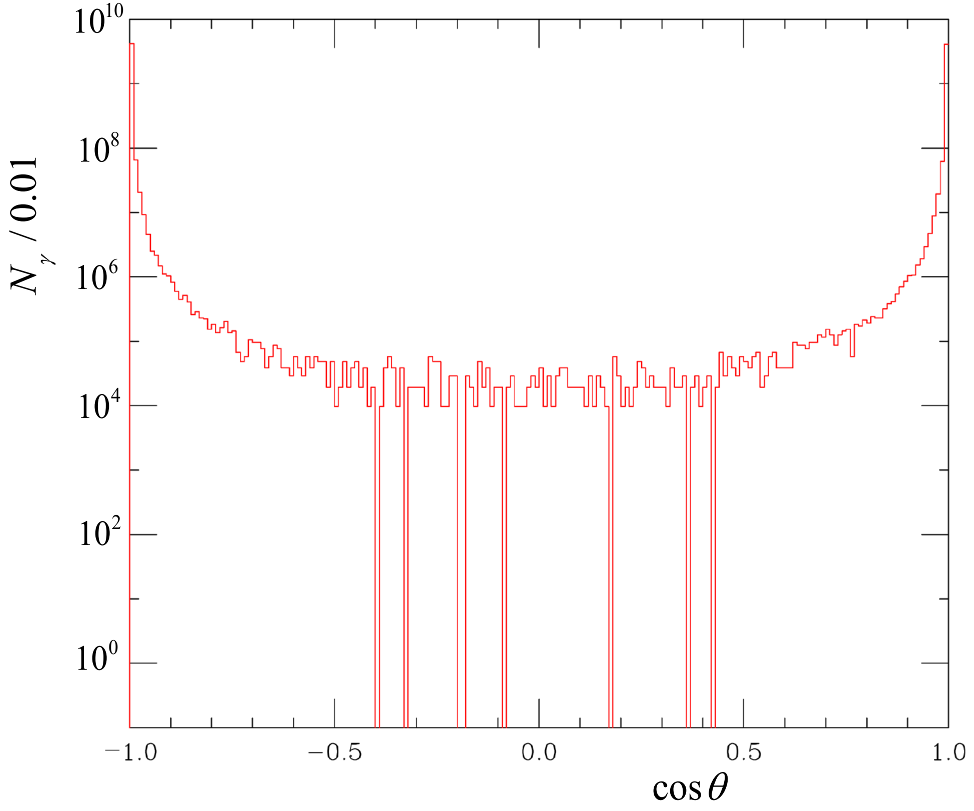

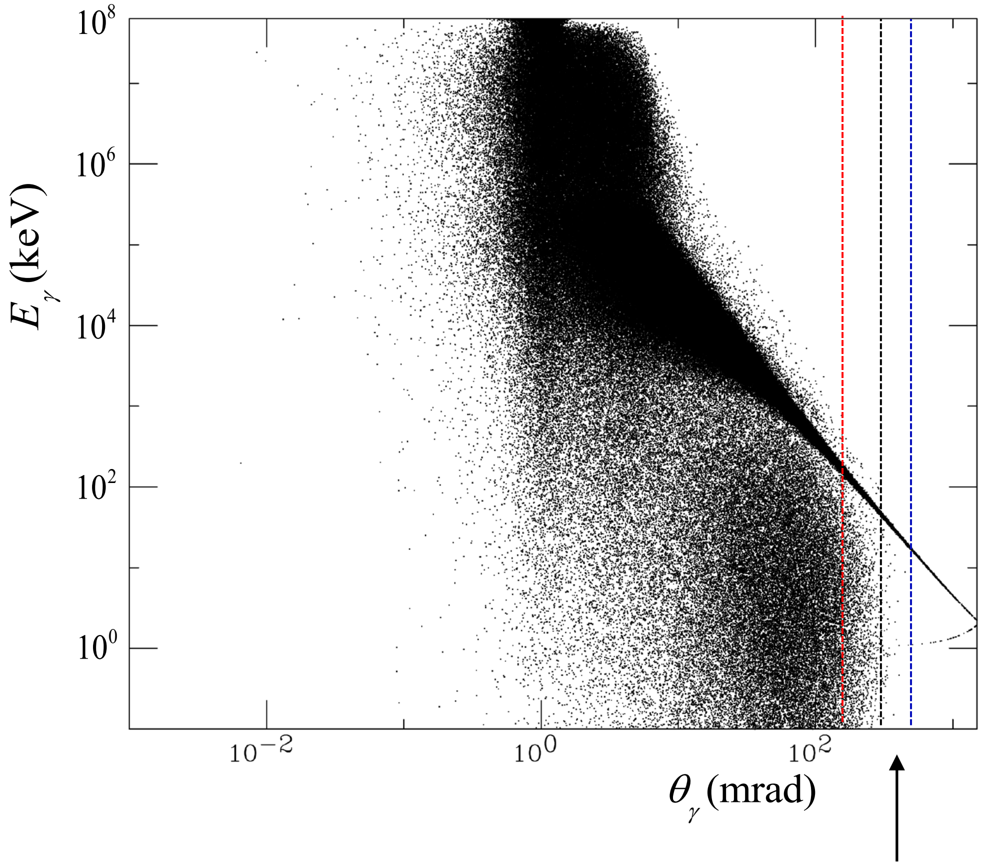

$|\cos\theta| = (0.99, 0.95, 0.90)$

X-rays handled by adding 0.1% - 1.0% X_0 heavy element to Beampipe for $|\cos\theta| < 0.8$

Required absorber increases to 5.0% X_0 at $|\cos\theta| = 0.93$

Complicated design for $0.95 < |\cos\theta| < 0.99$; probably can't instrument for $|\cos\theta| > 0.99$

$\gamma\gamma \to HH$ at $\sqrt{s} = 380$ GeV

- At 0.4 fb, the cross section for $\gamma\gamma \to HH$ at $\sqrt{s}$=380 GeV is twice that of $e^+e^- \to ZHH$ at $\sqrt{s}$=500 GeV, so that the XCC Higgs self-coupling measurement starts out with a $\sqrt{2}$ statistical advantage over 500 GeV e^+e^- colliders.

- The HH final state is simpler than ZHH. N.B., the associated Z boson in e^+e^- production of the Higgs is great for measurements such as Γ_{ZZ} & $\Gamma_{\text{invisible}}$, but can be a complication in other instances.

- Interesting interference between box diagram and s-channel: constructive at XCC vs. destructive at LHC

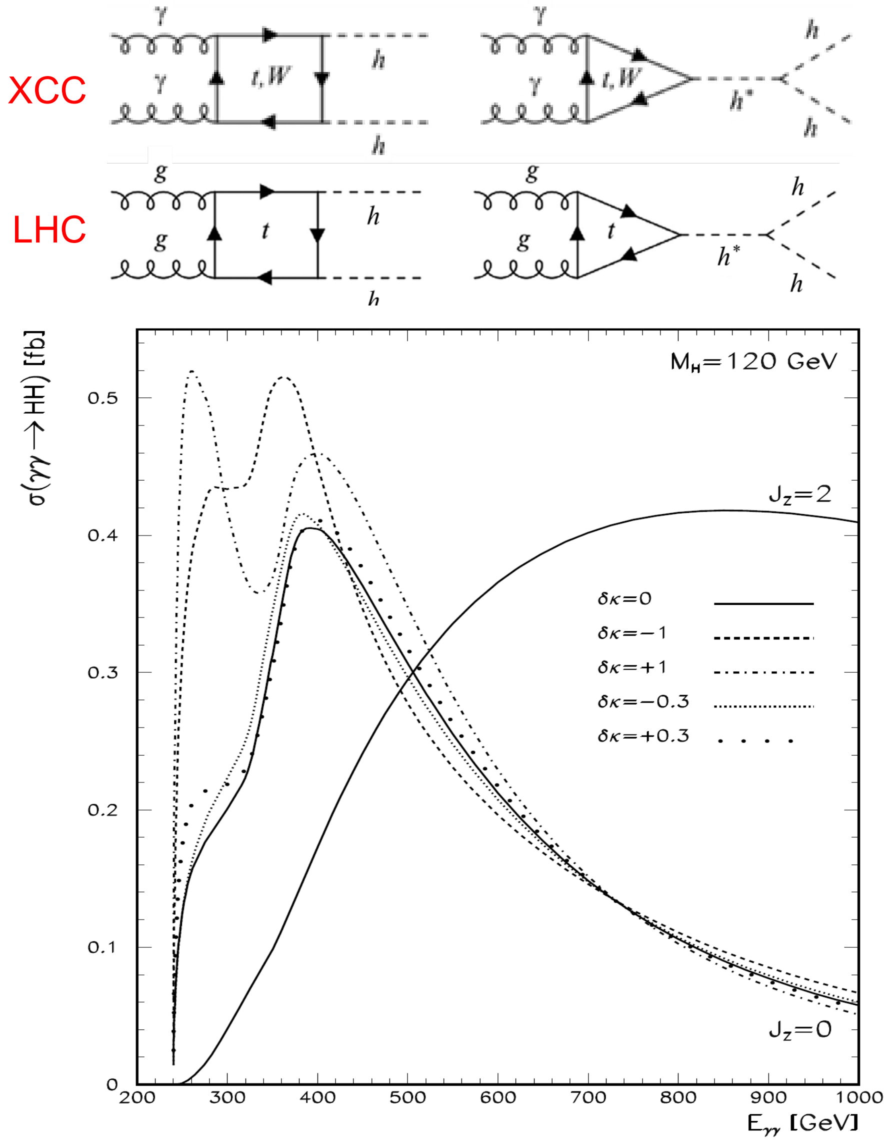

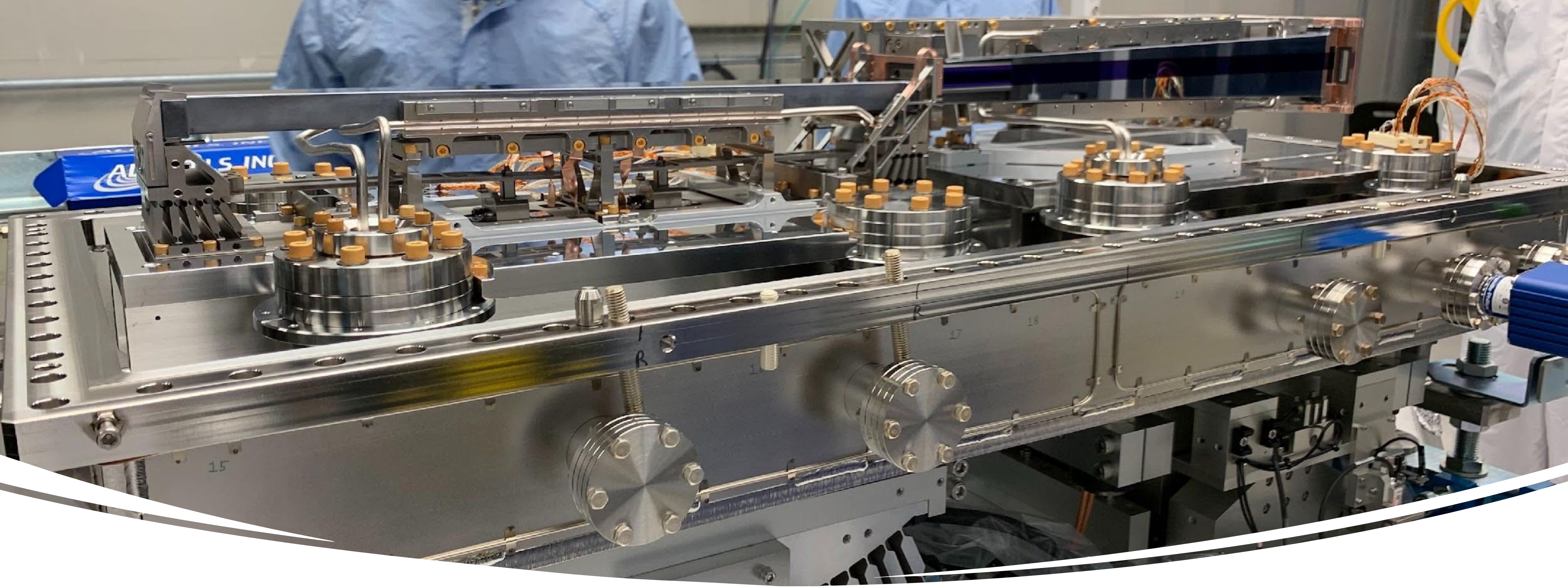

KB Mirror Focusing for $\gamma\gamma$ Collider

Some Possibilities for ≤70 nm FWHM Focal Size (Round Equivalent)

Focal Size (nm)	Photon Energy (eV)	Rayleigh Range (um)	RMS Source Size (um)	AOI (deg)	Max E w/ 10x SF (J)	Substrate Length (m)	Unfocused Beam Size (mm)	Source Distance (m)	Reflectivity	Focal Length (m)	IP Distance from Mirror (m)
50	1000	4.5	10	1.30	0.31	1.00	11.34	487	0.872	1.032	0.532
100	1000	18.2	10	0.90	0.68	1.50	11.78	505	0.926	2.144	1.394
50	2000	9.1	10	0.80	0.54	1.00	6.98	600	0.933	1.27	0.770
100	2000	36.4	10	0.60	1.05	1.40	7.33	629	0.967	2.668	1.968
50	2000	9.1	10	0.65	1.21	1.50	8.51	731	0.962	1.548	0.798
100	2000	36.4	10	0.50	2.14	2.00	8.73	750	0.976	3.176	2.176
40	4000	11.6	10	0.4	1.06	1.13	3.93	675	0.982	1.143	0.581
70	4000	35.7	10	0.3	2.40	1.50	3.93	675	0.992	2.001	1.251
40	4000	11.6	10	0.4	2.39	1.50	5.24	899	0.982	1.525	0.775
70	4000	35.7	10	0.3	4.27	2.00	5.24	899	0.992	2.668	1.668

- KB pairs are needed to focus the beam
- If source is round, then KB mirrors will create an elliptical focus
- Round equivalent = $\sqrt{vert * horizontal}$
- Things improve with photon energy for the KB optics: *(probably forces 1 keV → 2 keV)*
  - Damage
  - Reflectivity --> less absorbed power
  - Focal size
  - Rayleigh range

Summary of Initial $\gamma\gamma$ Collider KB Mirror Study

- Large mirrors (> 1 m) are needed for 1 J per pulse energy
  - 1 m FEL quality substrates produced today
  - 1.5 m substrates produced for synchrotrons
  - > 1 m FEL quality substrates would require development with industry but not R&D
- > 1 km source to KB optic distance is desirable
- FEL average power is a new regime (6.5 kW)
  - This requires an engineering study
  - Very grazing angles help since the most straight forward approach is to absorb less in the substrate
  - Another reason to consider beyond state-of-the-art substrates sizes (e.g. 2 m or beyond)

Final Quad Aperture

CAIN Simulation from IP to Face of Quad, Assume 5 T Solenoid